

Supporting Information-1

Multiple climate tipping points metrics for improved sustainability assessment of products and services

Serena Fabbri^{1*}, Michael Z. Hauschild¹, Timothy M. Lenton², Mikołaj Owsianiak¹

¹Quantitative Sustainability Assessment group, Department of Technology, Management and Economics, Technical University of Denmark, Produktionstorvet, Building 424, DK-2800 Kgs. Lyngby, Denmark.

²Global Systems Institute, University of Exeter, Exeter EX4 4QE, UK.

*Corresponding author

serf@dtu.dk

This file contains

Supporting Information text pages S1-S37

Figures S1-S6

Tables S1-S10

Table of Contents

S1. Supplementary methods

S1.1 Review and selection of climate tipping elements

S1.2 Calculation of *impact of the emission*, $I_{\text{emission},i,j}(T_{\text{emission}})$

S1.3 Calculation of capacity, $CAP_j(T_{\text{emission}})$

S1.3.1 Calculation of effects from tipping, $C_{\text{tip}}(t)$

S1.3.2 Notes on tipping elements for which C_{tip} was not modelled

S1.3.3 Atmospheric capacity cutoff

S1.4 Consideration of time as a variable

S1.5 Example calculation of MCTP with two tipping points

S1.6 Details of two illustrative simulations

S1.7 Calculation of impact scores for the case study

S2. Supplementary results

S2.1 Supplementary MCTP results

S2.2 Details and supplementary results for the case study

S3. References

37 **S1. Supplementary methods**

38 This section includes (i) review and selection of climate tipping elements, (ii) methods for calculation
39 of *impact of the emission*, capacity and effects from crossing tipping points (including justifications
40 when effects from tipping were not modelled), (iii) reasoning for setting a capacity cutoff, (iv) an
41 example of MCTP calculation with two tipping points, (v) details of the two illustrative simulations
42 presented in the main article and (vi) equations for calculation of impact scores with MCTP and the
43 other metrics used in the case study.

44

45 **S1.1 Review and selection of climate tipping elements**

46 The following three criteria were used to select relevant tipping elements in this study:

47

48 *Criterion 1: There is an evidence of a critical threshold beyond which a small change in one variable*
49 *controlling the system (control variable) causes a large qualitative change in the system (that is, the*
50 *system exhibits threshold behavior). The change may be abrupt and occur immediately after the cause*
51 *or gradual and spanning over longer timescales. This criterion excludes those tipping elements for*
52 *which the transition to a new state is a continuous process without strong nonlinearity or threshold*
53 *behavior. To ensure that there is minimum understanding of the tipping dynamics supported by*
54 *scientific evidence we considered only those tipping points, which are described in at least two studies*
55 *published by different groups in peer-reviewed journals. In cases where there were more studies but*
56 *the evidence of threshold behavior was debated between them, we conservatively assumed that the*
57 *potential tipping element does exhibit threshold behavior, thus meeting the criterion.*

58

59 *Criterion 2: There is an evidence that the system's critical control variable that may pass a threshold*
60 *is influenced by changes in atmospheric CO₂-equivalent GHGs concentration. This influence is*
61 *typically indirect, meaning that a change in GHG concentrations affects certain parameters that in turn*
62 *have an influence on the control variable of the system (e.g. GHG concentrations affect atmospheric*
63 *temperature, which, in turn, influences the freshwater and heat inputs that control the thermohaline*
64 *circulation in the North Atlantic). This criterion is chosen because climate tipping characterization*
65 *factors (CF) are for greenhouse gas emissions. Thus, those tipping points that cannot be related to*
66 *GHG concentrations, but are influenced by e.g. aerosol pollution, are not relevant and are therefore*
67 *excluded.*

68

69 *Criterion 3: Tipping threshold estimates and their relative uncertainties can be expressed as global*
70 *mean temperature change above pre-industrial levels. Despite relatively uncertain link between*
71 *global mean temperature and the actual control variable of a tipping element¹, global mean*
72 *temperature change is used here as indicator of threshold levels because it was found to be the most*

73 common way of reporting critical thresholds among studies (see references in Table S1). Thus, we
74 excluded tipping elements for which threshold estimations are only given based on local physical
75 parameters, e.g. sea ice extent/thickness, rate of ocean current or precipitation rate, for which the
76 calculation of the corresponding level of atmospheric GHGs concentration equivalents (i.e. the
77 concentration necessary to calculate the remaining capacity) is either not possible or highly uncertain.

78

79 An overview of all potential tipping elements is given in Table S1. Table S2 provides
80 an overview of potential occurrence of the 13 selected tipping elements under the considered
81 Representative Concentration Pathways (RCP).

82 **Table S1:** Overview of potential tipping elements from the literature and their fulfilment of the selection criteria (1, 2 and 3) in this study. Selected tipping
83 points that meet all criteria are highlighted in bold. When available, ranking based on likelihood is shown for illustrative purposes even though it was not used
84 as a criterion. Fulfilment of selection criteria is indicated with ‘y’ = yes; ‘n’ = no; ‘un’ = uncertain.

Tipping element	Critical tipping threshold ^a (global mean temperature above pre-industrial in °C, unless differently indicated)		Climatic triggering and main feedback mechanism	Transition period ^b (yr)		Likelihood		Fulfilled selection criteria		
		Reference			Reference	Relative likelihood ²	Likelihood with increasing global warming ³	1	2	3
Arctic summer sea ice loss (AS)	1.2 – 2.7 ^c	⁴	Melting of sea exposes larger areas of ocean surface to solar radiation, decreasing the albedo and increasing heat absorption by the ocean, thus amplify the warming. This loss of sea ice could lead to ice cap melting beyond certain size/thickness at which complete melting is likely to occur every summer.	10	⁴	1	1	y	y	y
	1 – 3	⁵								
	1.5 – 2 ^d	^{6, 7}								
	2.2 – 2.7 (2.5)	⁸								
Greenland ice sheet melt (GI)	1.7 – 2.7 ^c	⁴	Increased air temperatures cause surface ice melting, which lowers ice altitude and increases surface temperature (due to higher temperatures at lower elevation) causing further warming and melting (melt-elevation feedback) to a point beyond which there is net mass loss and GI shrinks radically ⁹ .	300 – 7500 (1500) ^c	¹⁰	2	2	y	y	y
	1 – 3	⁵								
	0.8 – 3.2 (1.6) ^e	¹¹								
	1.9 – 5.1 (3.1) ^e	¹²								
	2 – 3	¹³								
	2 – 4	¹⁴								
West Antarctic ice sheet collapse (AI)	3.7 – 5.7 ^c	⁴	The collapse is due to the combination of (i) surface melting (see GI) and (ii) the retreat of the submerged grounding line caused by the intrusion of warmer ocean water, which increases the ice flux and induces further retreat ^{3,9} .	100 – 2500 (500) ^c	¹⁰	3	4	y	y	y
	1 – 3	⁵								
	4 ^f	¹⁵								
	1 – 5.7	¹⁶								
Amazon rainforest dieback (AF)	3.7 – 4.7 ^c	⁴	Warmer temperatures cause reduction in precipitations, lengthening of the dry season and directly affect vegetation productivity, leading to forest dieback, which in turn further reduces precipitations ¹⁷ .	50 – 250 (50) ^c	¹⁰	3	3	y	y	y
	3 – 5	⁵								
	2.5, 6.2 ^g	¹⁸								
	2, 3, 4 ^h	¹⁷								
Sahara/Sahel and West African monsoon shift (AM)	3.7 – 4.7 ^c	⁴	Warming of sea surface temperature influences the direction of the West African monsoon, which in turn affects rainfall in the Sahara/Sahel region. It is uncertain whether WAS will shift northward (leading to increased rainfall) or southward (leading to further drying of the Sahel) ⁹ .	10	⁴	4	6	y	y	y
	3 – 5	⁵								
	2.1, 2.8, 3.5 ⁱ	¹⁸								

Boreal forest dieback (BF)	3.7 – 5.7 ^c	⁴	Increased water stress, peak summer heat stress, vulnerability to disease and fire frequency due to higher temperatures cause boreal forest dieback and transition to open woodlands or grasslands, which in turn would amplify summer heat stress, drying and fire frequency ³ .	50	⁴	5	4	y	y	y
	3 – 5	⁵								
El Niño-Southern Oscillation change in amplitude (EN)	3.7 – 6.7 ^c	⁴	Increased heat uptake in the equatorial Pacific could lead to a permanent deepening of the thermocline, which could result in more persistent El Niño-like conditions. However, it is not excluded that stronger warming of the west Equatorial Pacific than the east could lead to more persistent La Niña-like conditions ⁴ . Complex and uncertain mechanism.	100	⁴	5	5	y	y	y
	3 – 5	⁵								
Atlantic thermohaline circulation shutoff (TC)	3.7 – 5.7 ^c	⁴	Addition of freshwater in the North Atlantic (due to sea ice and Greenland ice sheet melting, river inputs and ocean precipitation) may reduce the density-driven sinking of North Atlantic waters until the Atlantic thermohaline circulation is significantly slowed down or even stopped ¹⁹ .	10 – 250 (50) ^c	¹⁰	5	5	y	y	y
	3 – 5	⁵								
	1.4, 1.6, 1.9 ⁱ	¹⁸								
	6 – 8 ⁱ	²⁰								
	1.4, 1.6, 2.2, 2.5 ¹	²¹								
Permafrost loss (P)	5.6	¹⁸	Thawing of permafrost (highly rich in organic carbon) in the northeastern Siberia (Yedoma) triggers biochemical decomposition of the organic matter, which generates heat that further increases warming and melting.	<100	⁴	Not assessed	7	y	y	y
	> 5	⁵								
	> 5	¹⁶								
Indian summer monsoon collapse	3 – 5	⁵	Monsoon dynamics depend on heat and pressure differences between land and ocean. Black carbon and aerosol emissions on land reduce land-absorbed solar radiation and the resulting lower warming of the land compared to the ocean weakens the monsoon to its eventual collapse. On the contrary, increased warming over land due to GHG emissions generally strengthens the monsoon. Increasing global average temperature influences the monsoon but does not lead to its collapse ¹⁹ .	1	⁴	Not assessed	Not assessed	y	n	y
Tundra loss	7.2	¹⁸	Warmer temperatures enable northward expansion of boreal forest in replacement of tundra regions, initiating a positive	100	⁴	Not assessed	Not assessed	y	y	n

			snow-albedo feedback where the darker surface covered with trees reduces snow albedo and amplifies warming.							
Marine methane hydrates release	-	-	Warmer ocean temperatures could melt the large amount of frozen methane hydrates and the gas bubbles they trap beneath sediments in the ocean floor, which would then be released in the atmosphere causing further warming ³ .	1000 – 100,000	⁴	Not assessed	Not assessed	y	y	n
Ocean anoxia	-	-	Warmer ocean temperatures decrease ventilation of deep water and solubility of O ₂ in surface water leading to widespread oceanic anoxic conditions. Low oxygen levels in the ocean increment the nitrous oxide emissions ²² and may have other consequences that could reduce ocean's CO ₂ absorption capacity ²³ .	10,000	⁴	Not assessed	Not assessed	y	y	n
Arctic ozone loss	-	-	“Global warming implies global cooling of the stratosphere that supports formation of ice clouds, which in turn provide a catalyst for stratospheric ozone destruction” ²⁴	1	⁴	Not assessed	Not assessed	un	y	n
Antarctic bottom water formation collapse	-	-	Increased precipitations at high latitudes resulting from global warming cause surface water freshening around Antarctica, which suppresses ocean convection and so bottom water formation ²⁵	≈ 100	⁴	Not assessed	Not assessed	un	y	n
Alpine glaciers loss (AG)	² 1 – 3	²⁶ ⁵	Increased temperatures cause reduction in snow and ice cover, originating a positive ice-albedo feedback, and prolongation of the melting season, which destabilizes the glacier mass balance towards glacier thinning and disintegration ²⁶	100	²⁶	Not assessed	Not assessed	y	y	y
Coral reefs deterioration (CR)	450 – 500 ppm [CO ₂] _{atm} 1 – 3 1.25 – 2 ^k	²⁷ ⁵ ²⁹	Increased sea temperature due to global warming results in coral bleaching (breakdown of symbiosis between corals and the algae that live inside their tissues) and mortality. Moreover, increased atmospheric CO ₂ concentration means higher uptake by oceans, where CO ₂ reacts to form carbonic acid, which reduces the availability of carbonate ions and the rate of calcification of corals ultimately favoring erosion. Both processes trigger multiple ecological feedback loops that eventually drive reefs to a non-coral dominated state ²⁷ .	few years to decades (<100)	²⁸	Not assessed	Not assessed	y	y	y

East Antarctic ice sheet collapse	>5	^{16,5}	Same dynamics as AI	200 – 800	³⁰	Not assessed	Not assessed	un	y	y
Arctic winter sea ice loss (AW)	4.5, 5.2, 6.2, 7.4, 8.2 ⁸	¹⁸	Besides ice-albedo feedback (see Arctic summer sea ice) also reduced ice thickness creates a positive feedback that leads to complete ice loss.	10	¹⁸	Not assessed	Not assessed	y	y	y
	>5	⁵								
North Atlantic subpolar gyre convection collapse (SG)	1.1, 1.4, 1.6, 1.7, 1.9, 2.0, 3.8 ¹	²¹	Warming and freshening of the North Atlantic subpolar gyre (an area of cyclonic ocean circulation in the Northwest Atlantic) leads to stratification (as consequence of lower surface density), that weakens the local deep convection, which in turn amplifies the stratification (because of reduced inflow of saltier water from the surroundings), eventually leading to permanent convection collapse. This collapse involves only the subpolar gyre (which is part of the TC) and not the whole North Atlantic TC.	10	¹⁸ ²¹	Not assessed	Not assessed	y	y	y
West tropical Indian oceanic bloom	10.9	¹⁸	“This event features an increase in equatorial upwelling, which is due to a general increase in oceanic velocity and divergence at the equator associated with enhanced wind stress at the surface linked to changes in monsoon regime. As a consequence of this increased divergence in the equatorial area, the upwelling increases, bringing a large amount of nutrients to the surface that are then advected toward the coast of Somalia, where the bloom is maximal” ¹⁸ .	≈ 10	¹⁸	Not assessed	Not assessed	n	un	n
Abrupt sea ice increase in Southern Ocean	1.6	¹⁸	Warming causes deep ocean convection to stop in the Indian sector of the Southern Ocean, which enables the formation of a fresh surface layer and hence of sea ice.	≈ 10	¹⁸	Not assessed	Not assessed	n	y	n
Abrupt Tibetan snow melt	1.4 – 2.2	¹⁸	Rising temperature “drives the system into a regime where the annual mass flux balance becomes negative and snow becomes a seasonal phenomenon” leading to a sudden loss of snow ¹⁸ .	≈ 10	¹⁸	Not assessed	Not assessed	n	y	y

85

^a Estimates are given as either intervals or single data points.

86

^b Time required for the full effect to unfold.

87

^c Data from Lenton et al.⁴ has been converted from 1980-1999 to 1850-1900 (pre-industrial) reference period by adding the average temperature change difference (0.7°C) between 1850-1900 and 1986-2005 periods found in the literature^{14,31} (Berkeley Earth global land and ocean data), assuming that the mean of 1980-1999 and 1986-2005 periods are not significantly different.

88

^d Projections do not refer to the range of global warming after which every Arctic summer will be ice free, but they represent the range of warming after which there is 30% (under 1.5°C) to 100% (under 2°C) probability of occurrence of at least an ice free summer by 2100. For example, at 2 degrees there is 100% probability that an ice-free summer will occur before 2100, but it is not a yearly recurring event. Thus, the

89

value does not indicate whether a shift to a different state (an ice-free state) has occurred.

90

91

^e Best estimate in brackets.

92

- 93 ^f Above 4°C it is more likely than not that the AI will collapse.
- 94 ^g Separate values obtained from different climate models under RCP8.5 assumptions.
- 95 ^h Thresholds above which around 20, 70 and 80% of dieback is inevitable, respectively.
- 96 ⁱ Separate values obtained with the same model under different RCP assumptions.
- 97 ^j Probability of TC collapse increases from 11% at 6°C warming to 30% at 8°C warming.
- 98 ^k Range at which more than 90% of reef cells are at risk of long-term degradation depending on the thermal tolerance of coral reefs.
- 99 ^l Separate values obtained from different climate models and emission scenario

100 **Arctic summer sea ice loss:** Future loss of Arctic summer sea ice has been extensively studied in the
101 literature (see for instance references ^{32,33,34}). Some authors argue that abrupt transition to summer ice-
102 free conditions is not likely based on the fact that the loss is in principle reversible^{35,36}. Others affirm
103 that irreversibility is not a prerequisite for being a tipping point and consider Arctic summer sea ice
104 loss as one of the first tipping points to be triggered as global temperature increases^{3,37,38}. Despite this
105 uncertainty, Arctic summer sea ice is conservatively assumed to be a tipping point in this study.

106

107 **West Antarctic ice sheet collapse:** Initial estimations place a potential threshold for AI collapse at
108 around 4°C warming or above. However, more recent studies highlight that AI might have already
109 started tipping^{39,40} even though no clear threshold range is indicated. Based on this, recent review
110 studies expanded the range with a potential threshold already at 1°C^{5,16}. All three criteria are met for
111 this tipping element.

112

113 **Permafrost loss:** Initial projections of permafrost melt did not show evidence of a critical threshold,
114 however recent work has suggested that at least one large area of permafrost could exhibit coherent
115 threshold behavior⁴¹⁻⁴³. Based on this, criterion 1 is met.

116

117 **Indian summer monsoon collapse:** Increasing global average temperature influences the monsoon
118 but does not lead to its collapse¹⁹, therefore the second criterion is not met.

119

120 **Tundra loss:** According to Lenton et al.⁴ tundra loss is not considered a tipping point because “the
121 transition from tundra to boreal forest is a continuous process without strong non-linearity or
122 threshold behavior”. However, a more recent study finds abrupt loss of tundra (in terms of roughly
123 70% boreal forest northward expansion in 100 years) at 7.2°C above pre-industrial, despite it is
124 acknowledged that tundra loss is a gradual transition¹⁸. Also Scheffer et al.⁴⁴ support the fact that
125 “climate change may invoke massive nonlinear shifts in boreal biomes” including tundra loss. Despite
126 the contrasting findings, it is conservatively decided that tundra loss does exhibit threshold behavior
127 and thus meets the first criterion. Threshold estimations in terms of global temperature change above
128 pre-industrial levels were found to be limited to the single value reported by ref. ¹⁸, with no
129 information about uncertainty. Due to this lack of uncertainty estimations, criterion three is not met.

130

131 **Marine methane hydrates release:** The release of methane via gas hydrate degradation is considered
132 a ‘slow’ tipping point leading to a long-term chronic release of methane on timescales of millennia
133 and longer⁴⁵. Due the length of the transition, this potential tipping point does not meet the definition
134 of ref. ⁴ because it is unlikely that qualitative changes in this Earth system will occur within this
135 millennium. Despite this, critical thresholds have been proposed suggesting that there is potential for

136 threshold behavior⁴⁵, thus meeting the first selection criterion. However, estimations are only based on
137 local parameters such as ocean temperature increase, thus criterion no. 3 is not met. In addition, it is
138 uncertain whether the released methane will actually reach the atmosphere in such amounts as to
139 significantly influence global GHGs concentration. Many biogeochemical sinks and physical
140 processes could prevent much of the gas from reaching the sea-air interface and being injected into
141 the atmosphere⁴⁶, with implications on quantification of effects on the global climate system.

142

143 ***Ocean anoxia***: Whether ocean anoxia represents an actual tipping point is still debated. While some
144 believe that anoxia events can lead to major regime shifts in relatively rapid time⁴⁷, others claim that a
145 shift to anoxic state requires too long periods (around 10000 years) for being considered a tipping
146 point⁴. Ocean anoxia is not considered an immediate climate change concern, however it is not
147 excluded that human-induced warming could increase nutrient weathering rates, which could cause
148 ocean anoxia (past ocean anoxia events are thought to be caused by global warming)⁴⁸. Even if
149 considering the phenomenon as a tipping point, criterion three is not met due to lack of threshold
150 estimations.

151

152 ***Arctic ozone loss***: It is currently unclear whether a tipping point exists for Arctic ozone^{24,26}. Feedback
153 mechanisms on the climate system due to a large-scale depletion of Arctic ozone are also poorly
154 described in the reviewed literature. According to Baldwin et al.⁴⁹, there are interactions between the
155 climate and the state of the ozone layer, e.g. as ozone is a greenhouse gas, its depletion could cause
156 cooling of the lower stratosphere. Overall, there is lack of evidence supporting that Arctic ozone loss
157 is a tipping element and no threshold estimations are reported (criterion 1 and 2 not met).

158

159 ***Antarctic bottom water formation collapse***: There is evidence that bottom water formation decreases
160 under climate change scenario simulations^{25,50-52}, however it is still not clear whether the phenomenon
161 has threshold behavior. As no threshold estimations were found, this potential tipping element does
162 not meet criterion 3.

163

164 ***Alpine glaciers loss***: Different model simulations of Alpine glacier extent demonstrate that an
165 increase in global mean air temperature of 2°C leads to an almost complete loss of glaciers in the
166 Alps⁵³⁻⁵⁵. Thus, Alpine glacier loss is selected as tipping element in our study.

167

168 ***Coral reefs deterioration***: There is agreement that rapid climate change and ocean acidification could
169 lead coral to the functional collapse of coral reefs^{16,27-29,56}. Despite this, some argue that it is still
170 unclear whether there is a large-scale tipping point⁴¹. Due to this uncertainty, coral reefs deterioration
171 is conservatively assumed to be a tipping element.

172
 173
 174
 175
 176
 177
 178
 179
 180
 181
 182
 183
 184
 185
 186
 187
 188
 189
 190
 191
 192

East Antarctic ice sheet collapse: Not enough evidence was found to conclude that the collapse of East Antarctic ice sheet could show threshold behavior. More research is needed to understand and quantify the potential as a major tipping element in the Earth's climate system⁵⁷.

Arctic winter sea ice loss: According to Kopp et al.⁵⁸, “the evidence that winter Arctic sea ice is a tipping element is stronger than for summer Arctic sea ice” and other authors found abrupt year-round ice loss in their simulations¹⁸ (meeting criterion 1).

North Atlantic Subpolar Gyre convection collapse: Some models forecast a collapse of the SG, where the deep convection in the Labrador sea shuts off in response to climatic conditions⁵⁹⁻⁶¹. In addition, two recent studies have identified the potential existence of a tipping point for the collapse of the SG^{18,21}. All three criteria are met for this element.

West tropical Indian oceanic bloom; Abrupt sea ice increase in Southern Ocean; Abrupt Tibetan snow melt: these potential abrupt events are described by only one of the reviewed studies¹⁸, hence the first selection criterion is not met. In addition, no uncertainty of threshold estimations are found for the first two candidates.

Table S2: Overview of selected tipping elements with relative temperature threshold intervals and their occurrence under the chosen RCP pathways.

Selected tipping element	Temperature threshold range [‡] (global mean temperature above pre-industrial level in °C)	Occurrence		
		RCP4.5	RCP6	RCP8.5
Arctic summer sea ice loss (AS)	1.5 – 2.6	Expected	Expected	Expected
Greenland ice sheet melt (GI)	1.6 – 3.5	Potential	Expected	Expected
West Antarctic ice sheet collapse (AI)	1.9 – 4.8	Potential	Potential	Expected
Amazon rainforest dieback (AF)	2.8 – 5.0	Potential	Potential	Expected
Boreal forest dieback (BF)	3.4 – 5.4	Not expected	Potential	Expected
El Niño-Southern Oscillation change in amplitude (EN)	3.4 – 5.9	Not expected	Potential	Expected
Permafrost loss (P)	5 – 8.5 [‡]	Not expected	Not expected	Expected
Arctic winter sea ice loss (AW)	4.8 – 8.2	Not expected	Not expected	Expected
Atlantic thermohaline circulation shutoff (TC)	3.1 – 4.6	Not expected	Potential	Expected

North Atlantic subpolar gyre convection collapse (SG)	1.2 [§] – 3.8	Potential	Expected	Expected
Sahara/Sahel and West African monsoon shift (AM)	2.9 – 4.4	Potential	Potential	Expected
Alpine glaciers loss (AG)	1.2 [§] – 3.0	Expected	Expected	Expected
Coral reefs deterioration (CR)	1.2 [§] – 2.5	Expected	Expected	Expected

193 † Assigned by taking the mean of the lower and upper bounds of available intervals following the approach in ref. ⁶², if not differently
194 specified.

195 § Literature data reports lower bounds (see Table S1), however 1.2°C was chosen arbitrarily to exclude the possibility that a tipping has
196 already been crossed.

197 ‡ As no specific upper bound is found (see Table S1), 8.5°C was chosen because it corresponds to the maximum temperature possibly
198 reachable under the selected RCP pathways within year 2500.

199
200
201

202 **S1.2 Calculation of the *impact of the emission*, $I_{\text{emission},i,j}(T_{\text{emission}})$**

203 Recall, that the *impact of the emission* for a chosen tipping point is calculated following the approach
204 in ref. ⁶³, and is renamed to the absolute climate tipping potential of gas i integrated between the
205 emission year T_{emission} and the year of tipping $T_{\text{tipping},j}$ ($ACTP_{i,j}(T_{\text{emission}})$) divided by the radiative
206 efficiency of 1 ppm CO₂ (RE_{CO_2}):

207

$$208 \quad I_{\text{emission},i,j}(T_{\text{emission}}) = \frac{ACTP_{i,j}(T_{\text{emission}})}{RE_{\text{CO}_2}} = \frac{\sum_{k=1}^n RF_i(T_{k-1}) \cdot \Delta T}{RE_{\text{CO}_2}} \quad (S1)$$

209

210 Where j indicates the j th tipping point occurring after the emission year and RF_i is the radiative
211 forcing of gas i . The radiative forcing is usually expressed (as a function of continuous time t) as the
212 product of the radiative efficiency of gas i (A_i) and the impulse response function (IRF), which for
213 most non-CO₂ GHGs is represented with a single exponential decay (eq. S2) and for CO₂ with a sum
214 of l exponentials (eq. S3)⁶⁴:

215

$$216 \quad RF_i(t) = A_i \cdot IRF_i(t) = A_i \left[e^{-\frac{t}{\tau_i}} \right] \quad (S2)$$

217

$$218 \quad RF_{\text{CO}_2}(t) = A_{\text{CO}_2} \cdot IRF_{\text{CO}_2}(t) = A_{\text{CO}_2} \left[a_0 + \sum_l a_l e^{-\frac{t}{\tau_l}} \right] \quad (S3)$$

219

220 The IRF describes the decay with continuous (and relative) time t of a perturbation in atmospheric
221 concentration of gas i after a pulse emission considering how quick the substance is removed from the
222 atmosphere. A summary of the different terms and parameters for calculation of the *impact of the*
223 *emission* is found in Tables S3, S4 and S5.

224 Radiative forcing function which was expressed as Riemann sum in eq. S1, can also be solved
 225 analytically (eq. S4 for a non-CO₂ gas i and eq. S5 for CO₂):
 226

$$227 \quad I_{\text{emission},i,j}(T_{\text{emission}}) = \frac{A_i \tau_i \left[1 - e^{-\frac{(T_{\text{tipping},j} - T_{\text{emission}})}{\tau_i}} \right]}{RE_{\text{CO}_2}} \quad (\text{S4})$$

$$228 \quad I_{\text{emission,CO}_2,j}(T_{\text{emission}}) = \frac{A_{\text{CO}_2} \left[a_0 (T_{\text{tipping},j} - T_{\text{emission}}) + \sum_l a_l \tau_l \left(1 - e^{-\frac{(T_{\text{tipping},j} - T_{\text{emission}})}{\tau_l}} \right) \right]}{RE_{\text{CO}_2}} \quad (\text{S5})$$

230
 231 As can be seen, for gas i the *impact of the emissions* occurring at different times is different as it
 232 depends on the distance between the emission year and the year of tipping.

233

234 **Table S3:** Overview of terms used in the calculation of $I_{\text{emission},i,j}(T_{\text{emission}})$.

Parameter	Name	Unit	Definition	Note
$I_{\text{emission},i,j}(T_{\text{emission}})$	Impact of the emission of gas i emitted at T_{emission} for the j th tipping point	ppm CO ₂ e · yr · kg ⁻¹	Time-integrated change in atmospheric CO ₂ -equivalent concentration due to a pulse emission of gas i from T_{emission} to $T_{\text{tipping},j}$	
$ACTP_{i,j}(T_{\text{emission}})$	Absolute Climate Tipping Potential of gas i	W · m ⁻² · yr · kg ⁻¹	Time-integrated radiative forcing due to a pulse emission of gas i from T_{emission} to $T_{\text{tipping},j}$	
j	-	-	Index for the sequence of occurring tipping points in a given iteration	An index taking numerical values was preferred rather than a qualifier for the subscript j , because the order of occurrence of tipping points can be different in different simulations
T_{emission}	Emission year (<i>interval time</i>)	yr	Any year starting from 2021 in which an emission can occur. T_{emission} indicates a specific time interval of 1 year.	See Table S7
t	Generic time (<i>point in time</i>)	yr	Continuous, point time expressed with real numbers	See Table S7
n	-	-	Number of time steps	Equal to the difference between the year

				of tipping $T_{\text{tipping},j}$ (i.e. the year when the j th tipping point is exceeded) and the year of emission, T_{emission} .
RF_{i/CO_2}	Radiative forcing	$\text{W} \cdot \text{m}^{-2} \cdot \text{kg}_i/\text{CO}_2^{-1}$	Radiative forcing due to a pulse emission of gas i/CO_2	
RE_{CO_2}	Radiative efficiency per ppm CO_2	$\text{W} \cdot \text{m}^{-2} \cdot \text{ppm CO}_2^{-1}$	Radiative forcing of 1 ppm CO_2 with a current background concentration of 409 ^a ppm	Reference value: $1.31 \cdot 10^{-2}$ (calculated based on ref. ⁶⁵).
IRF_{i/CO_2}	Impulse Response Function	unitless	Fraction of gas i/CO_2 remaining in the atmosphere at time t after a pulse emission	
A_i/CO_2	Radiative efficiency of gas i/CO_2	$\text{W} \cdot \text{m}^{-2} \cdot \text{kg}_i/\text{CO}_2^{-1}$	Radiative forcing per unit mass increase in atmospheric abundance of gas i/CO_2	See Table S4.
τ_i	Atmospheric lifetime (or adjustment time)	yr	Time scale characterizing the decay of a pulse emission input into the atmosphere ⁶⁶	Different from the lifetime of a gas, as it accounts for the effects of feedbacks resulting from a pulse emission ⁶⁷ . See Table S4.
a_l { $l=0,1,2,3$ }	-	unitless	Weight of each exponential	See Table S5.
τ_l { $l=1,2,3$ }	-	yr	Decay times of each exponential	See Table S5.
l	-	-	Number of exponentials	Up to 4

235 ^a Annual average of CO_2 in situ air measurements (February 2018 - January 2019) from Mauna Loa
236 Observatory, Hawaii⁶⁸.

237

238 **Table S4:** Radiative efficiency (A_i) and atmospheric lifetime (τ_i) for CO_2 , CH_4 and N_2O ⁶⁶. A_i values are
239 converted from $\text{W} \cdot \text{m}^{-2} \cdot \text{ppbv}_i^{-1}$ to $\text{W} \cdot \text{m}^{-2} \cdot \text{kg}_i^{-1}$ using previous methods⁶⁴.

	A_i ($\text{W} \cdot \text{m}^{-2} \cdot \text{kg}_i^{-1}$)	τ_i (yr)
CO_2	$1.67\text{E-}15^{\text{a}}$	-
CH_4	$1.82\text{E-}13^{\text{b}}$	12
N_2O	$3.87\text{E-}13$	114

240 ^a Obtained using the updated radiative efficiency per ppm of CO_2 (RE_{CO_2}) presented in Table S3 ($1.31 \cdot 10^{-2} \text{ W}$
241 $\text{m}^{-2} \cdot \text{ppm CO}_2^{-1}$).

242 ^b The calculation includes multiplication by a factor 1.4 to account for indirect radiative effects of methane
243 emissions⁶⁶.

244

245

246

247

248 **Table S5:** Constant parameter values for calculation of radiative forcing of CO₂ from ref. ⁶⁹.

Parameter	1 st term ($l=0$)	2 nd term ($l=1$)	3 rd term ($l=2$)	4 th term ($l=3$)
a_l (unitless)	2.123E-01 (a_0)	2.444E-01	3.360E-01	2.073E-01
τ_l (yr)	-	3.364E+02	2.789E+01	4.055E+00

249

250 **S1.3 Calculation of capacity, $CAP_j(T_{\text{emission}})$**

251 Recall, that the $CAP_j(T_{\text{emission}})$ (ppm CO₂e · yr) is given:

252
$$CAP_j(T_{\text{emission}}) = C(T_{\text{tipping},j}) \cdot (T_{\text{tipping},j} - T_{\text{emission}}) - \sum_{k=1}^n [C(T_{k-1}) + C_{\text{tip}}(T_{k-1})] \cdot \Delta T \quad (S6)$$

253 where, $C(T_{\text{tipping},j})$ is the atmospheric CO₂-equivalent concentration at the year of tipping $T_{\text{tipping},j}$,

254 $C(T)$ is the CO₂-equivalent concentration from background emissions at time T and $C_{\text{tip}}(T)$ is the

255 change in CO₂-equivalent concentration at time T caused by all tipping points occurred before

256 T_{emission} (all terms expressed in ppm CO₂e). Determination of $C(T_{\text{tipping},j})$ and $C(T)$ depends on the

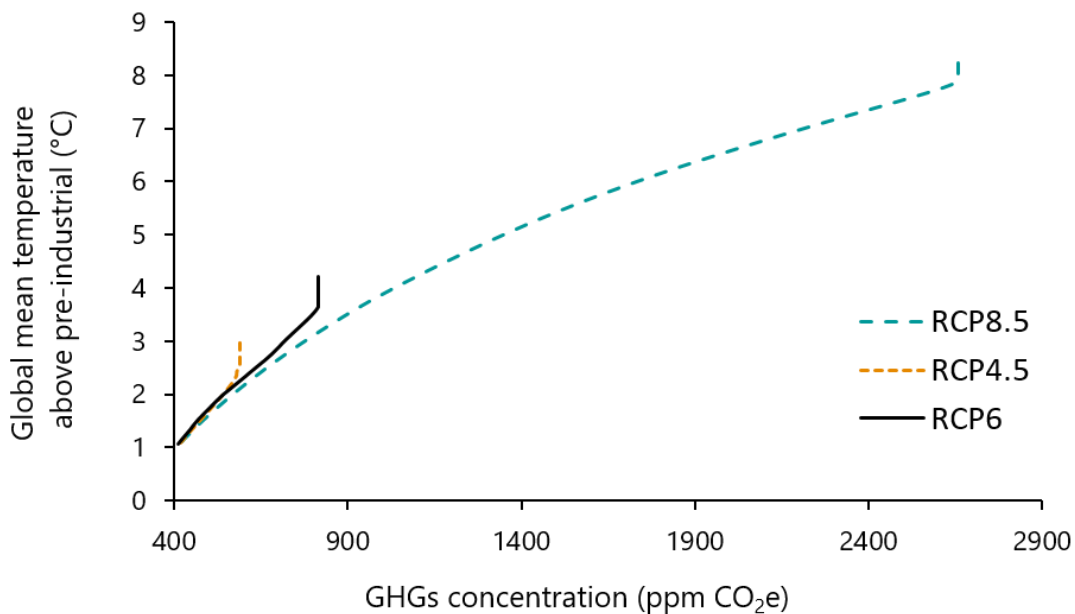
257 background development of GHG emissions as predicted by the RCP pathways. Differences in the

258 relationship between projected GHGs concentration and the corresponding equilibrium temperature

259 between the pathways (Figure S1) results in different remaining capacity to the same tipping point

260 when calculated with the three RCPs.

261



262

263 **Figure S1:** Relationship between projected GHGs concentration and temperature change in the chosen RCP

264 pathways.

265

266 ***S1.3.1 Calculation of effects from tipping, $C_{\text{tip}}(T)$***

267 $C_{\text{tip}}(T_{\text{effect}})$ is defined as the sum of the change in CO₂-equivalent concentration caused by all tipping
 268 points occurred before the emission year T_{emission} . T_{effect} is used here (rather than generic year T) to
 269 represent the year in which effects caused by all these tipping points unfold. The resulting overall
 270 effect from tipping is therefore expressed as a sum of effects of each tipping element (eq S7):

271

$$272 \quad C_{\text{tip}}(T_{\text{effect}}) = \sum_a C_{\text{tip},a}(T_{\text{effect}}) \quad (S7)$$

273

274 where a indicates a concrete tipping element that passed its tipping point before T_{emission} , and $C_{\text{tip},a}$
 275 is the CO₂-equivalent concentration increase caused by crossing the tipping point of the tipping
 276 element a . Here we use subscript a indicating a specific tipping element (e.g. a = Arctic summer sea
 277 ice loss), rather than subscript j because the effect from tipping depends on the tipping element being
 278 crossed and not on its order of occurrence.

279 For Arctic summer and winter sea ice loss (AS and AW), the effect from tipping is calculated
 280 based on the RF change due to reduced sea ice albedo (Table S6), which is then converted to annual
 281 concentration increase using the radiative efficiency of CO₂ per 1 ppm (found in Table S3). This
 282 effect is assumed to unfold completely from the year after tipping and to remain constant over the
 283 years, as the evolution of radiative forcing changes after tipping is unknown. Thus, at any year after
 284 tipping (T_{effect}), $C_{\text{tip},AS}$ and $C_{\text{tip},AW}$ are found to be 22.2 and 52.0 ppm CO₂e (Figure S2). For
 285 Greenland ice sheet melt (GI), West Antarctic ice sheet collapse (AI), El Niño-Southern Oscillation
 286 change in amplitude (EN), Permafrost loss (P), Amazon (AF) and Boreal forest (BF) tipping points, a
 287 dynamic (i.e. changing over time) effect (in terms of equivalent GHG concentration increase) was
 288 calculated by adapting the method used in Levasseur et al.⁷⁰. Estimates of carbon emissions that could
 289 be released after tipping (shown in Table S6) were used to calculate the dynamic effects, considering
 290 that all emitted carbon is in the form of CO₂, except for emissions from permafrost thawing or
 291 flooding, which are in the form of methane (CH₄). Considering the residence time of CO₂ and
 292 methane in the atmosphere, the instantaneous value of the dynamic characterization factor (expressed
 293 as time-integrated increase in CO₂-equivalent concentration) of a pulse emission at any year T after
 294 the emission was calculated as:

295

$$296 \quad DCF_{\text{inst},i}(T) = \int_{t_{\text{ini}}-1}^{t_{\text{ini}}} \Delta C_i \cdot IRF_i(t) \cdot \frac{RE_i}{RE_{\text{CO}_2}} dt \quad \text{for } T = 1, 2, 3, \dots \quad (S8)$$

297

298 where $DCF_{\text{inst},i}(T)$ is the instantaneous dynamic characterization factor of gas i computed for
 299 intervals of 1-year length (i.e. T = year 1, year 2, etc.), where the relative time interval T is defined

300 within $T = [t_{\text{ini}}, t_{\text{end}}]$, and where time t is relative and continuous. The ΔC_i ($\text{ppm}_i \cdot \text{kg}_i^{-1}$) is the
301 change in atmospheric GHG concentration due to a unit emission of gas i ; $IRF_i(t)$ is the impulse
302 response function of gas i representing the decay of the gas after a pulse emission (defined as in eq.
303 S2, for non- CO_2 gasses, and eq. S3, for CO_2); RE_i is the radiative efficiency per ppm of gas i (0.37 W
304 $\cdot \text{m}^{-2} \cdot \text{ppm}^{-1}$ for methane⁷¹) and RE_{CO_2} is the radiative efficiency per ppm CO_2 (see Table S3). Note
305 that $DCF_{\text{inst},i}$ is expressed as time-integrated increase in CO_2 -equivalent concentration ($\text{ppm CO}_2\text{e} \cdot \text{yr}$
306 $\cdot \text{kg}_i^{-1}$) and thus it deviates from the DCF expressed as time-integrated radiative forcing increase ($\text{W} \cdot$
307 $\text{m}^{-2} \cdot \text{yr} \cdot \text{kg}_i^{-1}$) calculated in Levasseur et al.⁷⁰. The ΔC_i was calculated as:

$$309 \quad \Delta C_i = \frac{1 \cdot 10^6 / M_i}{m_{\text{air}} / M_{\text{air}}} \cdot 1 \cdot 10^3 \quad (\text{S9})$$

310
311 Where M_i is the molar mass of gas i (16 and $44 \text{ g} \cdot \text{mol}^{-1}$ for CH_4 and CO_2 respectively); m_{air}
312 ($5.14 \cdot 10^{21} \text{ g}$) and M_{air} ($28.9 \text{ g} \cdot \text{mol}^{-1}$) are the total mass and the molar mass of air in the atmosphere
313 respectively⁷¹, $1 \cdot 10^6$ (ppm) and $1 \cdot 10^3$ ($\text{g} \cdot \text{kg}^{-1}$) are conversion factors. The instantaneous dynamic
314 characterization factor represents the annual value of the characterization factor of a pulse emission,
315 where the pulse emission is the annual amount of CO_2 or methane emissions caused by crossing a
316 tipping point. By combining the instantaneous dynamic characterization factor of one annual release
317 with the evolution of this annual release over the years, the dynamic effect at year T_{effect} was
318 obtained:

$$319 \quad C_{\text{tip},a}(T_{\text{effect}}) = \sum_i \sum_{T=T_a+1}^{T_{\text{effect}}} e_i(T) \cdot DCF_{\text{inst},i}(T_{\text{effect}} - T) \quad (\text{S10})$$

321
322 Where T_a is the year of tipping of the element a , $e_i(T)$ ($\text{kg}_i \cdot \text{yr}^{-1}$) is the annual release of gas i (either
323 CO_2 or methane depending on the tipping point) at year T , i.e. at any year before the year of
324 calculation of the dynamic effect (T_{effect}) since the year following the tipping ($T_a + 1$). The $e_i(T)$ is
325 determined by equally subdividing the estimated total carbon release after tipping (shown in Table
326 S6) over the transition period of the tipping event (i.e. time required for the full effect to unfold found
327 in Table S1). In this way, the time evolution of the annual release is assumed to be constant, meaning
328 that the same amount of emissions is released every year over the transition period. In the case of GI,
329 AI and Amazon forest, the transition period was also considered to calculate for how long this annual
330 release lasts (e.g. for Amazon tipping point annual release ceases after 50 years). For EN the
331 estimated release is basically permanent¹⁰, while for permafrost and Boreal forest 80 years of release

332 are assumed given that the figures used from ref. ⁵ refer to emissions from present day to 2100 (≈ 80
 333 years)⁵.

334 At any year after tipping (T_{effect}), the dynamic effect calculated through eq. S10 is the
 335 result of the emissions released at year T_{effect} and the non-decayed fraction of emissions that occurred
 336 in all previous years (T) since the year of tipping. The result provides the cumulative increase in CO₂-
 337 equivalent concentration at time T_{effect} caused by every discrete annual release occurred since the
 338 year after the tipping event until T_{effect} . Dynamic and constant (for Arctic summer and winter sea ice
 339 loss) effects from tipping used in this study are presented in Figure S2.

340

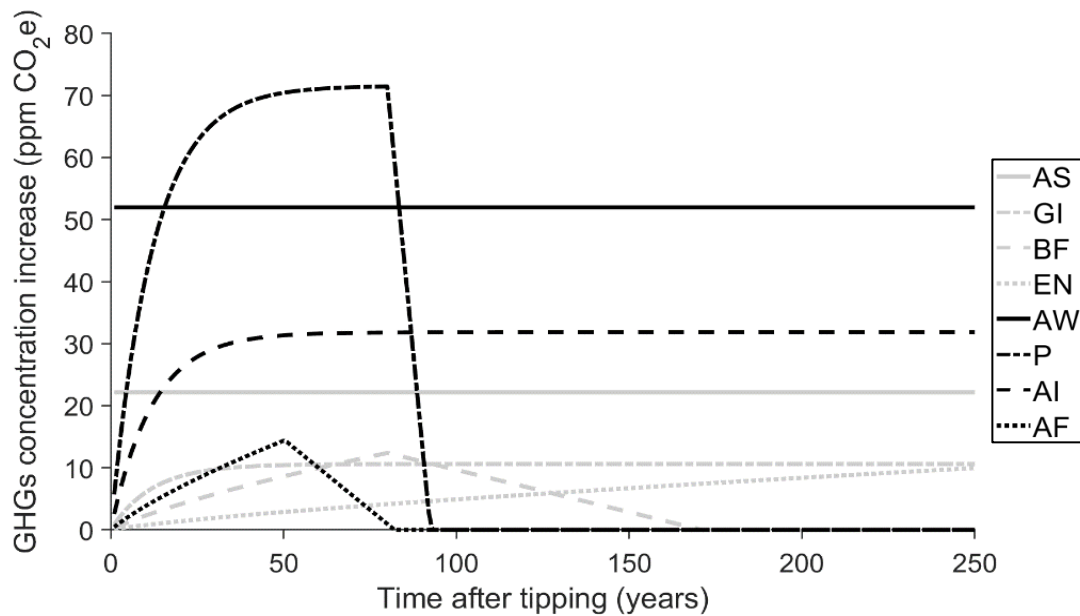
341 **Table S6:** Best available estimated consequences from tipping found in the literature used to calculate C_{tip} for 8
 342 tipping elements (no effect was modelled for the other tipping elements).

Selected tipping element	Estimated consequences from tipping		
	Amount	Unit	Definition
Arctic summer sea ice loss (AS)	0.29	$\text{W} \cdot \text{m}^{-2} \cdot \text{yr}^{-1}$	Total annual radiative forcing caused by one month of ice-free conditions, calculated from reduced sea-ice albedo effect ⁷² . In this study, the effect is assumed to unfold completely the year after tipping and to remain constant over time.
Greenland ice sheet melt (GI)	100	Gt C	Total carbon emissions, released over the transition period (best estimate 1500 years), from flooding of large areas of low-lying permafrost ¹⁰ .
West Antarctic ice sheet collapse (AI)	100	Gt C	Total carbon emissions, released over the transition period (best estimate 500 years), from flooding of large areas of low-lying permafrost ¹⁰ .
Amazon rainforest dieback (AF)	50	Gt C	Total carbon emissions, released over the transition period (best estimate 50 years), from forest dieback ¹⁰ .
Boreal forest dieback (BF)	10-40 (30)	Gt C	Estimated carbon emissions by 2100 ⁵ . In this study, it is assumed to be the total effect from tipping occurring over a transition period of 80 years.
El Niño-Southern Oscillation change in amplitude (EN)	0.2	$\text{Gt C} \cdot \text{yr}^{-1}$	Total annual carbon emissions released from anomalous fire events caused by stronger El Niño events. Assumed to be a permanent effect ¹⁰ .
Permafrost loss (P)	20-80 (45)	Gt C	Estimated carbon emissions by 2100 ⁵ . In this study, it is assumed to be the total effect from tipping occurring over transition period of 80 years.
Arctic winter sea ice loss (AW)	0.68	$\text{W} \cdot \text{m}^{-2} \cdot \text{yr}^{-1}$	Total annual radiative forcing caused by year-round ice-free conditions, calculated from reduced sea-ice albedo effect ⁷² . This effect is assumed to unfold completely the year after tipping and to remain constant over time.

343

344

345



346

347 **Figure S2:** Temporal evolution of CO₂-equivalent concentration increase caused by crossing eight of the
 348 selected tipping elements as modelled in this study. Uncertainty surrounding these results is undefined and thus
 349 not considered. AS = Arctic summer sea ice loss, GI = Greenland ice sheet melt, BF = Boreal forest dieback, EN
 350 = El Niño-Southern Oscillation change in amplitude, AW = Arctic winter sea ice loss, P = Permafrost loss, AI =
 351 West Antarctic ice sheet collapse, AF = Amazon rainforest dieback.

352

353 ***S1.3.2 Notes on tipping elements for which C_{tip} was not modelled***

354 ***Sahara/Sahel and West African monsoon shift (AM):*** It is uncertain whether AM will shift
 355 northward (leading to increased rainfall) or southward (leading to further drying of the Sahel)³. In
 356 either cases, modelling the consequences of a local change in rainfall on the global climate system
 357 remains challenging and no estimate allowing expressing the effect as a change in CO₂-equivalent
 358 concentration was found. Therefore, the effect from crossing this climate tipping point was not
 359 modelled.

360

361 ***Atlantic thermohaline circulation shutoff (TC) and North Atlantic Subpolar Gyre convection***
 362 ***collapse (SG):*** The main expected consequences of a potential Atlantic thermohaline circulation
 363 shutoff are cooling of the northern hemisphere and warming of the southern hemisphere^{21,73,74}. A
 364 collapse of the subpolar gyre convection would cause local cooling over the North Atlantic and, to a
 365 minor extent, over Western Europe and North American coast²¹. Some studies found that a collapse of
 366 both TC and SG would cause a reduction of the global mean temperature, leading to an overall
 367 cooling of the planet contrasting the global warming trend^{21,75}. However, no clear evidence of the
 368 underlying mechanism emerges from the studies and the same authors highlight that the observed
 369 cooling might be the result of factors such as the climate sensitivity parameter used in the models²¹.
 370 For this reason, no effect from these two tipping points is assumed in our model.

371
372
373
374
375
376
377
378
379
380
381
382
383
384
385
386
387
388
389
390
391
392
393
394
395
396
397
398
399
400

Alpine glaciers loss (AG): Shrinkage of Alpine glaciers and snow cover is expected to have mainly local effects, reducing surface reflectivity and thus leading to amplified temperature increase in the region²⁶. However, no estimate allowing expressing the effect as a change in global CO₂-equivalent concentration was found; therefore the effect from crossing this climate tipping point was not modelled.

Coral reefs deterioration (CR): Deterioration of coral reefs damages local marine habitats and species, causing loss of biodiversity²⁷, however it does not have direct or measurable consequences on the climate system, such as temperature increase due to positive feedbacks. Thus, the effect from crossing this climate tipping point was not accounted for.

S1.3.3 Atmospheric capacity cutoff

To define a meaningful minimum value for the atmospheric capacity (i.e. the value below which the difference between CO₂-equivalent concentrations is considered too small), the uncertainty surrounding the calculation of the capacity shall be quantified. The annual variability of atmospheric CO₂ concentrations, based on average in situ air measurements between 1959 – 2018 from Mauna Loa Observatory, Hawaii⁶⁸, was used as a proxy. The average difference in annual CO₂ concentrations was found to be 5.89 ppm CO₂, which was rounded to 6 ppm CO₂ because differences in annual measurements were not detected at decimal level. The cutoff was then applied to the difference between the concentration at the year of tipping and the concentration at year *T* when calculating the capacity as in eq. 4 in the main article.

Ideally, the uncertainty of future projections of GHGs concentrations should be used, as the capacity depends mainly on this parameter. However, when calculated from IPCC's temperature projections uncertainties⁷⁶, we found cutoff values between 43 – 70 ppm CO₂ equivalents, depending on the RCP pathway, which are deemed too high and were therefore not used. As a measure of the variability of GHGs concentration within the yearly time step used in the model, CO₂ was taken as a proxy because it is the most abundant anthropogenic greenhouse gas in the atmosphere.

401 **S1.4 Consideration of time as a variable**

402

403 **Table S7:** Summary of the symbols used to indicate the time variable in this paper.

Symbol	Meaning	Where it is used
T	<i>Interval-like</i> time variable indicating generic years that can be either <i>absolute</i> or <i>relative</i> .	In eq. 2, 3, 4, S1, S6, S8, S10.
t	<i>Point-like</i> time variable indicating continuous time that can be either <i>absolute</i> or <i>relative</i> .	In the standard definition of RF (eq. S2, S3) and as integration variable in eq. S8. Used also in Figure 1 as <i>absolute</i> variable.
T_{emission}	<i>Interval-like</i> and <i>absolute</i> time variable used to indicate <i>emission</i> years.	In all situations where the dependent variable is a function of the emission year and where years are intended as time intervals (eq. 1-4, S1 and S4-S6).
$T_{\text{tipping},j}$	<i>Interval-like</i> and <i>absolute</i> time variable indicating the year of tipping of the j th expected tipping point.	In eq. 3, 4, S4-S6.
T_{effect}	<i>Interval-like</i> and <i>absolute</i> time variable used to indicate the years after crossing tipping points, when <i>effects</i> of tipping unfold.	For calculation of the concentration increase from tipping C_{tip} (eq. S7 and S10).
$T_{\text{tipping},j_{\text{last}}}$	<i>Interval-like</i> and <i>absolute</i> time variable indicating the year of tipping of the last (j_{last}) expected tipping point across 10,000 Monte Carlo simulations.	As upper bound of the summation sign in eq. 5.
T_a	<i>Interval-like</i> and <i>absolute</i> time variable indicating the year of tipping of tipping element a (used for calculation of the effect from tipping). Subscript a is used rather than subscript j (as in $T_{\text{tipping},j}$), because the effect from tipping depends on the tipping element being crossed and not on its order of occurrence.	Used to define the lower bound of the summation in eq. S10

404

405

406 **S1.5 Example calculation of MCTP with two tipping points**

407 Figure 1 in the main article illustrates how the MCTP framework can be applied with two tipping
408 points. When considering the first tipping point ($j = 1$) occurring at year $T_{\text{tipping},1}$, every emission at
409 $T_{\text{emission}} < T_{\text{tipping},1}$ (before $T_{\text{tipping},1}$) takes up a certain part of the atmospheric capacity available
410 before reaching the concentration at the year of tipping $T_{\text{tipping},1}$ ($C(T_{\text{tipping},1})$). However, when
411 considering a second tipping point ($j = 2$) at year $T_{\text{tipping},2}$, the same emission $T_{\text{emission}} < T_{\text{tipping},1}$
412 will now take up also the capacity left before reaching the concentration at the second year of tipping
413 $T_{\text{tipping},2}$ ($C(T_{\text{tipping},2})$). Therefore, the total MCTP of gas i emitted at year $T_{\text{emission}} < T_{\text{tipping},1}$ is
414 given by the sum of the MCTPs for the first and the second tipping point (first and second term in eq.
415 S11 respectively). Assuming, hypothetically, $T_{\text{tipping},1} = 2030$, $T_{\text{tipping},2} = 2043$ and $T_{\text{emission}} <$
416 $T_{\text{tipping},1} = 2025$:

417

$$\begin{aligned}
418 \quad MCTP_i(2025) &= \frac{I_{\text{emission},i,1}(2025)}{CAP_1(2025)} + \frac{I_{\text{emission},i,2}(2025)}{CAP_2(2025)} = \frac{\left\{ \frac{A_i \tau_i \left[1 - e^{-\frac{(2030-2025)}{\tau_i}} \right]}{RE_{CO_2}} \right\}}{C(2030) \cdot (2030 - 2025) - \sum_{k=1}^5 [C(T_{k-1})] \cdot 1} \\
419 \quad &+ \frac{\left\{ \frac{A_i \tau_i \left[1 - e^{-\frac{(2043-2025)}{\tau_i}} \right]}{RE_{CO_2}} \right\}}{(2043) \cdot (2043 - 2025) - \sum_{k=1}^{18} [C(T_{k-1})] \cdot 1} \quad (S11)
\end{aligned}$$

420

421 where, each term of the sum is the ratio between the *impact of the emission* for either the first or the
422 second tipping point and the corresponding remaining capacity; A_i is the radiative efficiency of gas i
423 [$\text{W} \cdot \text{m}^{-2} \cdot \text{kg}_i^{-1}$]; τ_i is the atmospheric lifetime of gas i [yr] and RE_{CO_2} is the radiative efficiency per
424 ppm CO_2 [$\text{W} \cdot \text{m}^{-2} \cdot \text{ppm CO}_2^{-1}$]. Note, that the $C_{\text{tip}}(T)$ term is not included in eq. S11 because no
425 tipping point has been crossed yet in this case.

426 For an emission at $T_{\text{emission}} > T_{\text{tipping},1}$ (after $T_{\text{tipping},1}$), which will also take up part
427 of the capacity left before $T_{\text{tipping},2}$, but has no influence on $T_{\text{tipping},1}$, the total MCTP is given only
428 by the contribution to exceed the second tipping point (assuming $T_{\text{emission}} > T_{\text{tipping},1} = 2035$):

429

$$\begin{aligned}
430 \quad MCTP_i(2035) &= \frac{I_{\text{emission},i,2}(2035)}{CAP_2(2035)} \\
431 \quad &= \frac{\left\{ \frac{A_i \tau_i \left[1 - e^{-\frac{(2040-2035)}{\tau_i}} \right]}{RE_{CO_2}} \right\}}{(2040) \cdot (2040 - 2035) - \sum_{k=1}^5 [C(T_{k-1}) + C_{\text{tip}}(T_{k-1})] \cdot 1} \quad (S12)
\end{aligned}$$

432

433 Here, the tipping point occurring at $T_{\text{tipping},1}$ has an effect on the climate system (C_{tip}) that further
434 reduces the remaining capacity up to the following year of tipping and anticipating tipping from 2043
435 to 2040 (so that $T_{\text{tipping},2} = 2040$). This is also accounted for in the calculation of the capacity.

436 While for both emissions at $T_{\text{emission}} < T_{\text{tipping},1}$ and $T_{\text{emission}} > T_{\text{tipping},1}$ the *impact of the*
437 *emission* depends on the residence time of the gas in the atmosphere and the difference between the
438 emission year and the year of tipping, the capacity varies depending on i) the difference in
439 atmospheric CO_2 -equivalent concentration between the emission year and the year of tipping and ii)
440 on timing of emissions. For emissions at $T_{\text{emission}} < T_{\text{tipping},1}$ (eq. S11), the effect from tipping (C_{tip})
441 is equal to zero as no tipping points have been crossed yet and therefore the total remaining capacity
442 for these emissions is not affected. On the contrary, for emissions at $T_{\text{emission}} > T_{\text{tipping},1}$ (eq. S12),
443 the remaining capacity is influenced by the C_{tip} from the crossed level.

444

445 **S1.6 Details of two illustrative simulations**

446 This section gives an overview on occurrence of tipping points in the two illustrative simulations
 447 presented in the main article and shows typical trends for *impacts of the emission* and remaining
 448 capacities in the calculation of MCTPs (taking as example simulation 1).

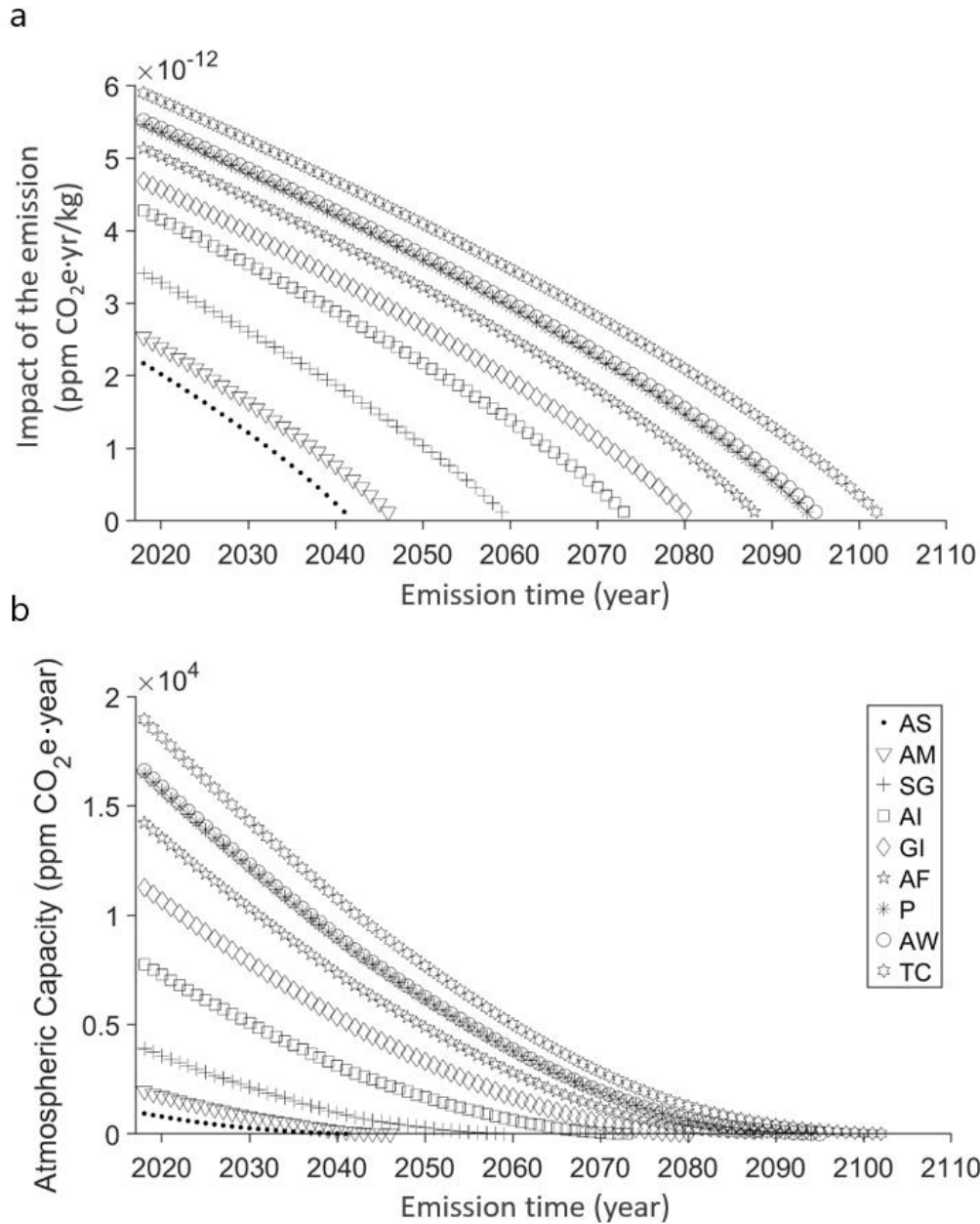
449

450 **Table S8:** Data on tipping points triggered in simulation 1 and simulation 2.

	Triggered tipping points (from first to last)	Threshold temperature (°C above pre-industrial)	Concentration at year of tipping (ppm CO _{2e})	Anticipated year of tipping (year)	Year of tipping without C_{tip} (year)
Simulation 1	Arctic summer sea ice loss	1.62	484	2042	2042
	West African monsoon shift	1.87	523	2047	2054
	North Atlantic subpolar gyre convection collapse	2.17	576	2060	2065
	West Antarctic ice sheet collapse	2.59	652	2074	2078
	Greenland ice sheet melt	2.95	711	2081	2092
	Amazon rainforest dieback	3.23	755	2089	2107
	Permafrost loss	3.41	784	2095	2119
	Arctic winter sea ice loss	3.42	786	2096	2120
	Atlantic thermohaline circulation shutoff	3.75	814	2103	2165
Simulation 2	Arctic summer sea ice loss	1.95	535	2056	2056
	West African monsoon shift	2.17	576	2060	2065
	Greenland ice sheet melt	2.30	600	2065	2069
	North Atlantic subpolar gyre convection collapse	2.40	617	2067	2072
	Arctic winter sea ice loss	2.59	652	2073	2078
	Atlantic thermohaline circulation shutoff	3.34	773	2100	2114
	Permafrost loss	4.02	814	2116	2298

451

452



453

454 **Figure S3:** (a) *Impact of the emission* of 1 kg CO₂ and (b) remaining atmospheric capacity relative to each of
 455 the 9 tipping points triggered in simulation 1. Both *impacts* and remaining capacities decrease over time, but
 456 capacities decrease faster than the *impacts*, explaining why MCTPs increase while approaching a tipping point.

457 AS = Arctic summer sea ice loss, AM = West African monsoon shift, SG = North Atlantic subpolar gyre
 458 convection collapse, AI = West Antarctic ice sheet collapse, GI = Greenland ice sheet melt, AF = Amazon
 459 rainforest dieback, P = Permafrost loss, AW = Arctic winter sea ice loss, TC = Atlantic thermohaline circulation
 460 shutoff.

461

462

463

464

465 **S1.7 Calculation of impact scores for the case study**

466

467 **Table S9:** Overview of equations used for calculation of impact scores (*IS*) with all metrics used in this study.

468 For all metrics, *i* denotes a specific GHG and T_{emission} the emission year. Note that the original notation for the
 469 time variable of the GWP-based and GTP CFs was harmonized with the notation used in this paper.

	Impact score calculation	Symbols
MCTP [ppt _{trc} /kg plastic]	$IS_{\text{MCTP}} = \sum_i \sum_{T_{\text{emission}}=2021}^{T_{\text{tipping},j_{\text{last}}}} m_i(T_{\text{emission}}) \cdot MCTP_i(T_{\text{emission}})$	$T_{\text{tipping},j_{\text{last}}}$ = year of last tipping point; $m_i(T_{\text{emission}})$ = mass of gas <i>i</i> emitted at year T_{emission} [kg]; $MCTP_i(T_{\text{emission}})$ = MCTP for gas <i>i</i> and emission year T_{emission} [ppt _{trc} · kg ⁻¹]
GWP20 [kg CO ₂ eq/kg plastic]	$IS_{\text{GWP20}} = \sum_i M_i \cdot GWP20_i$	M_i = total mass of gas <i>i</i> emitted in 20 years [kg]; $GWP20_i$ = GWP20 of gas <i>i</i> [kg CO ₂ eq · kg ⁻¹]
GWP100 [kg CO ₂ eq/kg plastic]	$IS_{\text{GWP100}} = \sum_i M_i \cdot GWP100_i$	M_i = total mass of gas <i>i</i> emitted in 100 years [kg]; $GWP100_i$ = GWP100 of gas <i>i</i> [kg CO ₂ eq · kg ⁻¹]
GWP100 _{ILCD} [kg CO ₂ eq/kg plastic]	$IS_{\text{GWP100ILCD}} = \sum_i M_i \cdot GWP100_i - Credit_i$ $Credit_i = \sum_{T=2}^{100} m_i(T) \cdot T \cdot EQ_i$	$Credit_i$ = ILCD credit for carbon storage; $m_i(T)$ = mass of gas <i>i</i> emitted at relative time <i>T</i> ; EQ_i = equivalency factor for gas <i>i</i> (0.01, 0.34 and 0.36 [kg CO ₂ eq · kg ⁻¹ · yr ⁻¹] for CO ₂ , biogenic and fossil CH ₄ respectively ^{77,78})
Dynamic GWP100 [kg CO ₂ eq/kg plastic]	$IS_{\text{dynGWP100}} = \frac{GWI_{\text{cum}}(100)}{\int_0^{100} A_{\text{CO}_2} \cdot C(t)_{\text{CO}_2} dt}$ $GWI_{\text{cum}}(100) = \sum_{T=0}^{100} GWI_{\text{inst}}(T)$ $GWI_{\text{inst}}(100) = \sum_i \sum_{T=0}^{100} m_i(T) \cdot DFC_i(100 - T)$ $DFC_i(100) = \int_{t-1}^{100} A_i \cdot C(t)_i dt$	$GWI_{\text{cum}}(100)$ = cumulative global warming impact in 100 years [W · m ⁻² · yr · kg ⁻¹]; A_{i/CO_2} = radiative efficiency per unit mass gas <i>i</i> /CO ₂ increase [W · m ⁻² · kg ⁻¹]; T = relative <i>interval</i> time [yr]; t = relative <i>point in time</i> [yr]; $C(t)_{i/\text{CO}_2}$ = atmospheric load of gas <i>i</i> /CO ₂ at time <i>t</i> after emission [kg]; $GWI_{\text{inst}}(100)$ = instantaneous global warming impact in 100 years [W · m ⁻² · yr · kg ⁻¹]; DFC_i = dynamic characterization factor of gas <i>i</i> [W · m ⁻² · yr]; (see equations 1-4 in Levasseur et al. ⁷⁹)
GTP100 [kg CO ₂ eq/kg plastic]	$IS_{\text{GTP100}} = \sum_i M_i \cdot GTP100_i$	M_i = total mass of gas <i>i</i> emitted over 100 years [kg]; $GTP100_i$ = GTP100 of gas <i>i</i> [kg CO ₂ eq · kg ⁻¹]

470

471

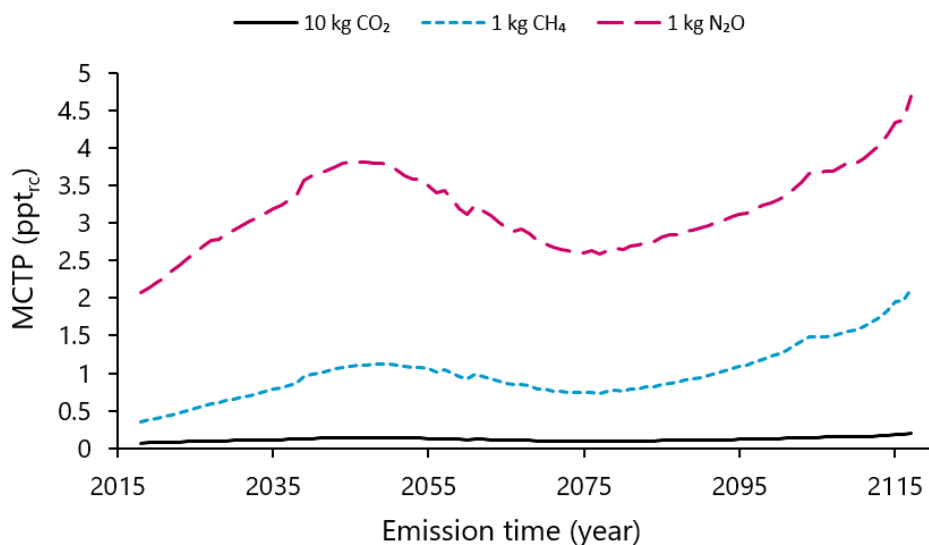
472 **S2. Supplementary results**

473 Sub-section S2.1 contains additional figures comparing average MCTP results for the three major
474 anthropogenic GHGs (carbon dioxide (CO₂), methane (CH₄) and nitrous oxide (N₂O)) and without
475 considering the effects from tipping. In sub-section S2.2, we show details on the case study,
476 comparing emission profiles with MCTP values and presenting MCTP impact scores calculated under
477 different RCP pathways.

478

479 **S2.1 Supplementary MCTP results**

480

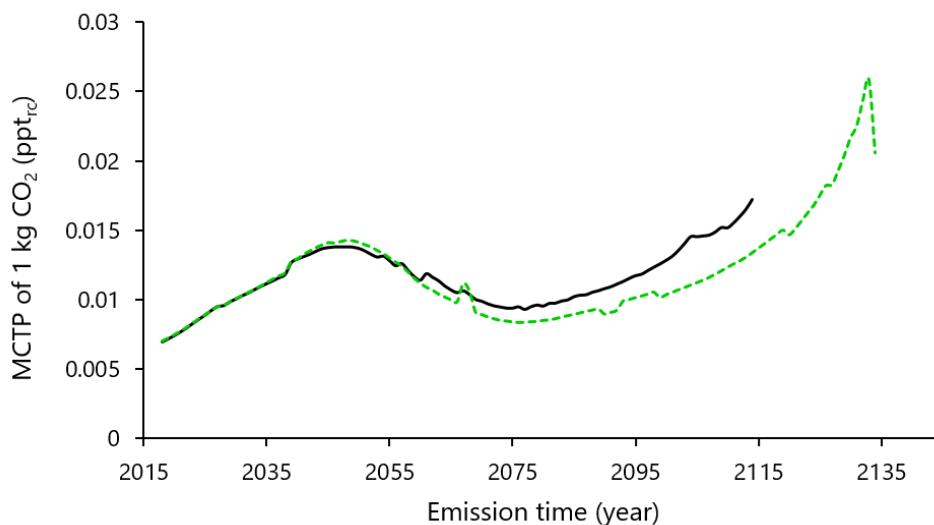


481

482 **Figure S4:** Average (geometric mean) multiple climate tipping points potential (MCTP) of CO₂, CH₄ and N₂O
483 at different emission years under RCP6 pathway. Note that results for CO₂ are given for 10 kg rather than 1 kg.

484

485



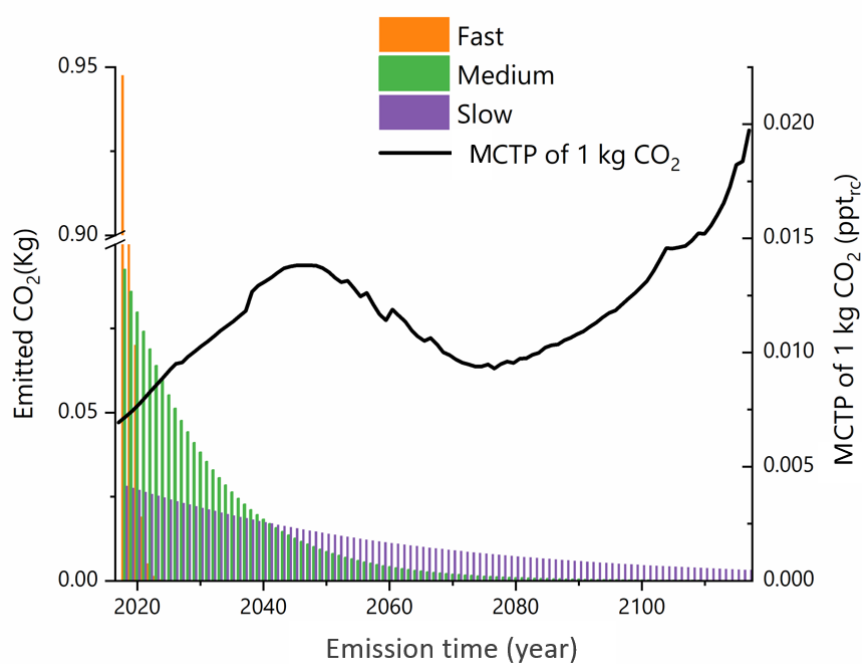
486

487 **Figure S5:** Average (geometric mean) multiple climate tipping points potential (MCTP) of 1 kg CO₂ under
488 RCP6 considering effects from crossing tipping points (black solid line) and without considering such effects
489 (green dashed line).

490

491 S2.2 Details and supplementary results for the case study

492



493

494 **Figure S6:** CO₂ emission profile for fast, medium and slow degrading plastics under anaerobic conditions (left
495 axis) and multiple climate tipping points potential (MCTP) per unit CO₂ emission (right axis).

496

497 **Table S10:** Climate tipping impact scores for different end-of-life degradation scenarios of plastic polymers
 498 calculated assuming background concentration pathways RCP4.5, RCP6 and RCP8.5. Ranking between
 499 scenarios 1 – 7 is illustrated within each column with different colors. Red shading indicates the highest impact
 500 scores and green the lowest impact scores.

End-of-life degradation scenario	MCTP - under RCP4.5 (ppt _{rc} /kg plastic)	MCTP - under RCP6 (ppt _{rc} /kg plastic)	MCTP - under RCP8.5 (ppt _{rc} /kg plastic)
1. Incineration ^a	0.015	0.014	0.014
Plastic degradation rate ^b			
2. Fast ^c	0.12	0.089	0.11
3. Medium ^d	0.22	0.14	0.17
4. Slow ^e	0.25	0.16	0.13
5. Very slow ^f	0.0027	0.0020	0.0011
Delayed degradation ^g			
6. After 20 years (fast rate)	0.31	0.21	0.24
7. After 50 years (fast rate)	0.45	0.16	0.15

501 ^aIncineration of fossil-based plastic where all carbon is emitted as CO₂ in the first year. ^bDegradation under
 502 anaerobic conditions. ^c90% degradation of polycaprolactone (PCL) in 2 years⁸⁰. ^d90% degradation of
 503 polybutylene succinate (PBS) in 31 years⁸¹. ^e90% degradation of polystyrene (PS) in 105 years⁸². ^f1%
 504 degradation of bio-based PLA in 100 years⁸³. ^gPotential short (20 years) and long (50 years) lag phase in
 505 degradation based on ref. ⁸³.

506 **S3. References**

507

- 508 (1) Lenton, T. M. Beyond 2°C: Redefining Dangerous Climate Change for Physical Systems.
509 *Wiley Interdiscip. Rev. Clim. Chang.* **2011**, 2 (3), 451–461. <https://doi.org/10.1002/wcc.107>.
- 510 (2) Lenton, T. M. Early Warning of Climate Tipping Points. *Nat. Clim. Chang.* **2011**, 1 (4), 201–
511 209. <https://doi.org/10.1038/nclimate1143>.
- 512 (3) Lenton, T. M. Future Climate Surprises. In *The Future of the World's Climate*; Henderson-
513 Sellers, A., McGuffie, K., Eds.; Elsevier B.V., 2012; pp 489–507.
- 514 (4) Lenton, T. M.; Held, H.; Kriegler, E.; Hall, J. W.; Lucht, W.; Rahmstorf, S.; Schellnhuber, H.
515 J. Tipping Elements in the Earth's Climate System. *Proc. Natl. Acad. Sci.* **2008**, 105 (6),
516 1786–1793. <https://doi.org/10.1073/pnas.0705414105>.
- 517 (5) Steffen, W.; Rockström, J.; Richardson, K.; Lenton, T. M.; Folke, C.; Liverman, D.;
518 Summerhayes, C. P.; Barnosky, A. D.; Cornell, S. E.; Crucifix, M.; Donges, J. F.; Fetzer, I.;
519 Lade, S. J.; Scheffer, M.; Winkelmann, R.; Schellnhuber, H. J. Trajectories of the Earth
520 System in the Anthropocene. *Proc. Natl. Acad. Sci.* **2018**, 115 (33), 8252–8259.
521 <https://doi.org/10.1073/pnas.1810141115>.
- 522 (6) Sigmond, M.; Fyfe, J. C.; Swart, N. C. Ice-Free Arctic Projections under the Paris Agreement.
523 *Nat. Clim. Chang.* **2018**, 8 (5), 404–408. <https://doi.org/10.1038/s41558-018-0124-y>.
- 524 (7) Jahn, A. Reduced Probability of Ice-Free Summers for 1.5 °c Compared to 2 °c Warming. *Nat.*
525 *Clim. Chang.* **2018**, 8 (5), 409–413. <https://doi.org/10.1038/s41558-018-0127-8>.
- 526 (8) Iseri, Y.; Yoshikawa, S.; Kiguchi, M.; Tawatari, R.; Kanae, S.; Oki, T. Towards the
527 Incorporation of Tipping Elements in Global Climate Risk Management: Probability and
528 Potential Impacts of Passing a Threshold. *Sustain. Sci.* **2018**, 13 (2), 315–328.
529 <https://doi.org/10.1007/s11625-018-0536-7>.
- 530 (9) Good, P.; Bamber, J.; Halladay, K.; Harper, A. B.; Jackson, L. C.; Kay, G.; Kruijt, B.; Lowe, J.
531 A.; Phillips, O. L.; Ridley, J.; Srokosz, M.; Turley, C.; Williamson, P. Recent Progress in
532 Understanding Climate Thresholds. *Prog. Phys. Geogr. Earth Environ.* **2018**, 42 (1), 24–60.
533 <https://doi.org/10.1177/0309133317751843>.
- 534 (10) Cai, Y.; Lenton, T. M.; Lontzek, T. S. Risk of Multiple Interacting Tipping Points Should
535 Encourage Rapid CO₂emission Reduction. *Nat. Clim. Chang.* **2016**, 6 (5), 520–525.
536 <https://doi.org/10.1038/nclimate2964>.
- 537 (11) Robinson, A.; Calov, R.; Ganopolski, A. Multistability and Critical Thresholds of the

- 538 Greenland Ice Sheet. *Nat. Clim. Chang.* **2012**, 2 (6), 429–432.
539 <https://doi.org/10.1038/nclimate1449>.
- 540 (12) Gregory, J. M.; Huybrechts, P. Ice-Sheet Contributions to Future Sea-Level Change. *Philos.*
541 *Trans. R. Soc. A Math. Phys. Eng. Sci.* **2006**, 364 (1844), 1709–1731.
542 <https://doi.org/10.1098/rsta.2006.1796>.
- 543 (13) Vizcaino, M.; Mikolajewicz, U.; Ziemen, F.; Rodehacke, C. B.; Greve, R.; Van Den Broeke,
544 M. R. Coupled Simulations of Greenland Ice Sheet and Climate Change up to A.D. 2300.
545 *Geophys. Res. Lett.* **2015**, 42 (10), 3927–3935. <https://doi.org/10.1002/2014GL061142>.
- 546 (14) Myhre, G.; Shindell, D.; Bréon, F.-M.; Collins, W.; Fuglestvedt, J.; Huang, J.; Koch, D.;
547 Lamarque, J.-F.; Lee, D.; Mendoza, B.; Nakajima, T.; Robock, A.; Stephens, G.; Takemura,
548 T.; Zhang, H. Anthropogenic and Natural Radiative Forcing. In *Climate Change 2013: The*
549 *Physical Science Basis. Contribution of Working Group I to the Fifth Assessment Report of the*
550 *Intergovernmental Panel on Climate Change.* Cambridge University Press; Stocker, T. F., Qin,
551 D., Plattner, G.-K., Tignor, M., Allen, S. K., Boschung, J., Nauels, A., Xia, Y., Bex, V.,
552 Midgley, P. M., Eds.; Cambridge University Press, Cambridge, United Kingdom and New
553 York, NY, USA., 2013.
- 554 (15) Kriegler, E.; Hall, J. W.; Held, H.; Dawson, R.; Schellnhuber, H. J. Imprecise Probability
555 Assessment of Tipping Points in the Climate System. *Proc. Natl. Acad. Sci.* **2009**, 106 (13),
556 5041–5046. <https://doi.org/10.1073/pnas.0809117106>.
- 557 (16) Schellnhuber, H. J.; Rahmstorf, S.; Winkelmann, R. Why the Right Climate Target Was
558 Agreed in Paris. *Nat. Clim. Chang.* **2016**, 6 (7), 649–653.
559 <https://doi.org/10.1038/nclimate3013>.
- 560 (17) Jones, C.; Lowe, J.; Liddicoat, S.; Betts, R. Committed Terrestrial Ecosystem Changes Due to
561 Climate Change. *Nat. Geosci.* **2009**, 2 (7), 484–487. <https://doi.org/10.1038/ngeo555>.
- 562 (18) Drijfhout, S.; Bathiany, S.; Beaulieu, C.; Brovkin, V.; Claussen, M.; Huntingford, C.; Scheffer,
563 M.; Sgubin, G.; Swingedouw, D. Catalogue of Abrupt Shifts in Intergovernmental Panel on
564 Climate Change Climate Models. *Proc. Natl. Acad. Sci.* **2015**, 112 (43), E5777–E5786.
565 <https://doi.org/10.1073/pnas.1511451112>.
- 566 (19) US CCCEF. *Climate Tipping Points : Current Perspectives and State of Knowledge*; 2009.
- 567 (20) Bakker, P.; Schmittner, A.; Lenaerts, J. T. M.; Abe-Ouchi, A.; Bi, D.; van den Broeke, M. R.;
568 Chan, W. L.; Hu, A.; Beadling, R. L.; Marsland, S. J.; Mernild, S. H.; Saenko, O. A.;
569 Swingedouw, D.; Sullivan, A.; Yin, J. Fate of the Atlantic Meridional Overturning Circulation:

- 570 Strong Decline under Continued Warming and Greenland Melting. *Geophys. Res. Lett.* **2016**,
571 43 (23), 12,252–12,260. <https://doi.org/10.1002/2016GL070457>.
- 572 (21) Sgubin, G.; Swingedouw, D.; Drijfhout, S.; Mary, Y.; Bennabi, A. Abrupt Cooling over the
573 North Atlantic in Modern Climate Models. *Nat. Commun.* **2017**, 8, 1–12.
574 <https://doi.org/10.1038/ncomms14375>.
- 575 (22) Arévalo-Martínez, D. L.; Kock, A.; Löscher, C. R.; Schmitz, R. A.; Bange, H. W. Massive
576 Nitrous Oxide Emissions from the Tropical South Pacific Ocean. *Nat. Geosci.* **2015**, 8 (7),
577 530–533. <https://doi.org/10.1038/ngeo2469>.
- 578 (23) Kwon, E. Y.; Primeau, F.; Sarmiento, J. L. The Impact of Remineralization Depth on the Air-
579 Sea Carbon Balance. *Nat. Geosci.* **2009**, 2 (9), 630–635. <https://doi.org/10.1038/ngeo612>.
- 580 (24) Lenton, T. M. Arctic Climate Tipping Points. *Ambio* **2012**, 41 (1), 10–22.
581 <https://doi.org/10.1007/s13280-011-0221-x>.
- 582 (25) Bi, D.; Budd, W. F.; Hirst, A. C.; Wu, X. Collapse and Reorganisation of the Southern Ocean
583 Overturning under Global Warming in a Coupled Model. *Geophys. Res. Lett.* **2001**, 28 (20),
584 3927–3930. <https://doi.org/10.1029/2001GL013705>.
- 585 (26) Levermann, A.; Bamber, J. L.; Drijfhout, S.; Ganopolski, A.; Haeberli, W.; Harris, N. R. P.;
586 Huss, M.; Krüger, K.; Lenton, T. M.; Lindsay, R. W.; Notz, D.; Wadhams, P.; Weber, S.
587 Potential Climatic Transitions with Profound Impact on Europe. *Clim. Change* **2012**, 110 (3–
588 4), 845–878. <https://doi.org/10.1007/s10584-011-0126-5>.
- 589 (27) Hoegh-Guldberg, O.; Harvell, C. D.; Sale, P. F.; Edwards, a J.; Caldeira, K.; Knowlton, N.;
590 Eakin, C. M. Coral Reefs under Rapid Climate Change and Ocean Acidification. *Science* (80-
591). **2007**, 318 (December 2007), 1737–1742. <https://doi.org/10.1126/science.1152509>.
- 592 (28) Veron, J. E. N.; Hoegh-Guldberg, O.; Lenton, T. M.; Lough, J. M.; Obura, D. O.; Pearce-
593 Kelly, P.; Sheppard, C. R. C.; Spalding, M.; Stafford-Smith, M. G.; Rogers, A. D. The Coral
594 Reef Crisis: The Critical Importance of <350 Ppm CO₂. *Mar. Pollut. Bull.* **2009**, 58 (10),
595 1428–1436. <https://doi.org/10.1016/j.marpolbul.2009.09.009>.
- 596 (29) Frieler, K.; Meinshausen, M.; Golly, A.; Mengel, M.; Lebek, K.; Donner, S. D.; Hoegh-
597 Guldberg, O. Limiting Global Warming to 2C Is Unlikely to Save Most Coral Reefs. *Nat.*
598 *Clim. Chang.* **2013**, 3 (2), 165–170. <https://doi.org/10.1038/nclimate1674>.
- 599 (30) Mengel, M.; Levermann, A. Ice Plug Prevents Irreversible Discharge from East Antarctica.
600 *Nat. Clim. Chang.* **2014**, 4 (6), 451–455. <https://doi.org/10.1038/nclimate2226>.

- 601 (31) Cowtan, K.; Way, R. G. Coverage Bias in the HadCRUT4 Temperature Series and Its Impact
602 on Recent Temperature Trends. *Q. J. R. Meteorol. Soc.* **2014**, *140* (683), 1935–1944.
603 <https://doi.org/10.1002/qj.2297>.
- 604 (32) Overland, J. E.; Wang, M. When Will the Summer Arctic Be Nearly Sea Ice Free? *Geophys.*
605 *Res. Lett.* **2013**, *40* (10), 2097–2101. <https://doi.org/10.1002/grl.50316>.
- 606 (33) Stein, R.; Fahl, K.; Schreck, M.; Knorr, G.; Niessen, F.; Forwick, M.; Gebhardt, C.; Jensen, L.;
607 Kaminski, M.; Kopf, A.; Matthiessen, J.; Jokat, W.; Lohmann, G. Evidence for Ice-Free
608 Summers in the Late Miocene Central Arctic Ocean. *Nat. Commun.* **2016**, *7*.
609 <https://doi.org/10.1038/ncomms11148>.
- 610 (34) Snape, T. J.; Forster, P. M. Decline of Arctic Sea Ice: Evaluation and Weighting of CMIP5
611 Projections. *J. Geophys. Res. Atmos.* **2014**, *119*, 546–554.
612 <https://doi.org/10.1002/2013JD020593>.
- 613 (35) Eisenman, I.; Wettlaufer, J. S. Nonlinear Threshold Behavior during the Loss of Arctic Sea
614 Ice. *Proc. Natl. Acad. Sci.* **2009**, *106* (1), 28–32. <https://doi.org/10.1073/pnas.0806887106>.
- 615 (36) Tietsche, S.; Notz, D.; Jungclaus, J. H.; Marotzke, J. Recovery Mechanisms of Arctic Summer
616 Sea Ice. *Geophys. Res. Lett.* **2011**, *38* (2), 1–4. <https://doi.org/10.1029/2010GL045698>.
- 617 (37) Holland, M. M.; Bitz, C. M.; Tremblay, B. Future Abrupt Reductions in the Summer Arctic
618 Sea Ice. *Geophys. Res. Lett.* **2006**, *33* (23), 1–5. <https://doi.org/10.1029/2006GL028024>.
- 619 (38) Smedsrud, L. H.; Sorteberg, A.; Kloster, K. Recent and Future Changes of the Arctic Sea-Ice
620 Cover. *Geophys. Res. Lett.* **2008**, *35* (20), 1–5. <https://doi.org/10.1029/2008GL034813>.
- 621 (39) Joughin, I.; Smith, B. E.; Medley, B. Marine Ice Sheet Collapse Potentially Under Way for the
622 Thwaites Glacier Basin, West Antarctica. *Science* (80-.). **2014**, *344* (May), 735–738.
- 623 (40) Rignot, E.; Mouginot, J.; Morlighem, M.; Seroussi, H.; Scheuchl, B. Widespread, Rapid
624 Grounding Line Retreat of Pine Island, Thwaites, Smith, and Kohler Glaciers, West
625 Antarctica, from 1992 to 2011. *Geophys. Res. Lett.* **2014**, *41* (10), 3502–3509.
626 <https://doi.org/10.1002/2014GL060140>.
- 627 (41) Lenton, T. M. Tipping Elements from a Global Perspective. In *Addressing Tipping Points for a*
628 *Precarious Future*; 2013; pp 23–46.
- 629 (42) Khvorostyanov, D. V.; Krinner, G.; Ciais, P.; Heimann, M.; Zimov, S. A. Vulnerability of
630 Permafrost Carbon to Global Warming. Part I: Model Description and Role of Heat Generated
631 by Organic Matter Decomposition. *Tellus, Ser. B Chem. Phys. Meteorol.* **2008**, *60 B* (2), 250–

- 632 264. <https://doi.org/10.1111/j.1600-0889.2007.00333.x>.
- 633 (43) Khvorostyanov, D. V.; Ciais, P.; Krinner, G.; Zimov, S. A. Vulnerability of East Siberia's
634 Frozen Carbon Stores to Future Warming. *Geophys. Res. Lett.* **2008**, *35* (10), 1–5.
635 <https://doi.org/10.1029/2008GL033639>.
- 636 (44) Scheffer, M.; Hirota, M.; Holmgren, M.; Van Nes, E. H.; Chapin, F. S. Thresholds for Boreal
637 Biome Transitions. *Proc. Natl. Acad. Sci.* **2012**, *109* (52), 21384–21389.
638 <https://doi.org/10.1073/pnas.1219844110>.
- 639 (45) Archer, D.; Buffett, B.; Brovkin, V. Ocean Methane Hydrates as a Slow Tipping Point in the
640 Global Carbon Cycle. *Proc. Natl. Acad. Sci.* **2009**, *106* (49), 20596–20601.
641 <https://doi.org/10.1073/pnas.0800885105>.
- 642 (46) Ruppel, C. D.; Kessler, J. D. The Interaction of Climate Change and Methane Hydrates. *Rev.*
643 *Geophys.* **2017**, *55* (1), 126–168. <https://doi.org/10.1002/2016RG000534>.
- 644 (47) Bush, T.; Diao, M.; Allen, R. J.; Sinnige, R.; Muyzer, G.; Huisman, J. Oxic-Anoxic Regime
645 Shifts Mediated by Feedbacks between Biogeochemical Processes and Microbial Community
646 Dynamics. *Nat. Commun.* **2017**, *8* (1). <https://doi.org/10.1038/s41467-017-00912-x>.
- 647 (48) Watson, A. J.; Lenton, T. M.; Mills, B. J. W. Ocean Deoxygenation, the Global Phosphorus
648 Cycle and the Possibility of Human-Caused Large-Scale Ocean Anoxia. *Philos. Trans. R. Soc.*
649 *A Math. Phys. Eng. Sci.* **2017**, *375* (2102). <https://doi.org/10.1098/rsta.2016.0318>.
- 650 (49) Baldwin, M. P.; Dameris, M.; Shepherd, T. G. How Will the Stratosphere Change Affect
651 Climate Change? *Science* (80-.). **2007**, *316* (5831), 1576–1577.
652 <https://doi.org/10.1126/science.1144303>.
- 653 (50) Marsland, S.; Bi, D.; Uotila, P.; Fiedler, R.; Griffies, S.; Lorbacher, K.; O'Farrell, S.; Sullivan,
654 A.; Uhe, P.; Zhou, X.; Hirst, A. Evaluation of ACCESS Climate Model Ocean Diagnostics in
655 CMIP5 Simulations. *Aust. Meteorol. Oceanogr. J.* **2013**, *63* (1), 101–119.
656 <https://doi.org/10.22499/2.6301.007>.
- 657 (51) Menezes, V. V.; Macdonald, A. M.; Schatzman, C. Accelerated Freshening of Antarctic
658 Bottom Water over the Last Decade in the Southern Indian Ocean. *Sci. Adv.* **2017**, *3* (1), 1–10.
659 <https://doi.org/10.1126/sciadv.1601426>.
- 660 (52) Rugenstein, M.; Sedláček, J.; Knutti, R. Nonlinearities in Patterns of Long Term Ocean
661 Warming. *Geophys. Res. Lett.* **2016**, *43*, 1–9.
- 662 (53) Zemp, M.; Haeberli, W.; Hoelzle, M.; Paul, F. Alpine Glaciers to Disappear within Decades?

- 663 *Geophys. Res. Lett.* **2006**, 33 (13). <https://doi.org/10.1029/2006GL026319>.
- 664 (54) Le Meur, E.; Gerbaux, M.; Schäfer, M.; Vincent, C. Disappearance of an Alpine Glacier over
665 the 21st Century Simulated from Modeling Its Future Surface Mass Balance. *Earth Planet. Sci.*
666 *Lett.* **2007**, 261 (3–4), 367–374. <https://doi.org/10.1016/j.epsl.2007.07.022>.
- 667 (55) Jouvét, G.; Huss, M.; Blatter, H.; Picasso, M.; Rappaz, J. Numerical Simulation of
668 Rhonegletscher from 1874 to 2100. *J. Comput. Phys.* **2009**, 228 (17), 6426–6439.
669 <https://doi.org/10.1016/j.jcp.2009.05.033>.
- 670 (56) McNeil, B. I.; Matear, R. J. Southern Ocean Acidification: A Tipping Point at 450-Ppm
671 Atmospheric CO₂. *Proc. Natl. Acad. Sci.* **2008**, 105 (48), 18860–18864.
672 <https://doi.org/10.1073/pnas.0806318105>.
- 673 (57) Fogwill, C. J.; Golledge, N. R.; Hillman, H.; Turney, C. S. M. The East Antarctic Ice Sheet as
674 a Source of Sea- Level Rise: A Major Tipping Element in the Climate System? *PAGES Mag.*
675 **2016**, 24 (1), 8–9. <https://doi.org/10.22498/pages.24.1.8>.
- 676 (58) Kopp, R. E.; Shwom, R. L.; Wagner, G.; Yuan, J. Tipping Elements and Climate–Economic
677 Shocks: Pathways toward Integrated Assessment. *Earth's Futur.* **2016**, 4 (8), 346–372.
678 <https://doi.org/10.1002/2016EF000362>.
- 679 (59) Levermann, A.; Born, A. Bistability of the Atlantic Subpolar Gyre in a Coarse-Resolution
680 Climate Model. *Geophys. Res. Lett.* **2007**, 34 (24), 1–6.
681 <https://doi.org/10.1029/2007GL031732>.
- 682 (60) Born, A.; Levermann, A. The 8.2 Ka Event: Abrupt Transition of the Subpolar Gyre toward a
683 Modern North Atlantic Circulation. *Geochemistry, Geophys. Geosystems* **2010**, 11 (6), 1–8.
684 <https://doi.org/10.1029/2009GC003024>.
- 685 (61) Lenton, T. M.; Ciscar, J.-C. Integrating Tipping Points into Climate Impact Assessments.
686 *Clim. Change* **2013**, 117 (3), 585–597. <https://doi.org/10.1007/s10584-012-0572-8>.
- 687 (62) Gioia, F.; Lauro, C. N. Basic Statistica Methods for Interval Data. *Stat. Appl. - Ital. J. Appl.*
688 *Stat.* **2005**, 17 (1).
- 689 (63) Jørgensen, S. V.; Hauschild, M. Z.; Nielsen, P. H. Assessment of Urgent Impacts of
690 Greenhouse Gas Emissions - The Climate Tipping Potential (CTP). *Int. J. Life Cycle Assess.*
691 **2014**, 19 (4), 919–930. <https://doi.org/10.1007/s11367-013-0693-y>.
- 692 (64) Shine, K. P.; Fuglestedt, J. S.; Hailemariam, K.; Stuber, N. Alternatives to the Global
693 Warming Potential for Comparing Climate Impacts of Emissions of Greenhouse Gases. *Clim.*

- 694 *Change* **2005**, 68, 281–302.
- 695 (65) Myhre, G.; Shindell, D.; Bréon, F.-M.; Collins, W.; Fuglestedt, J.; Huang, J.; Koch, D.;
696 Lamarque, J.-F.; Lee, D.; Mendoza, B.; Nakajima, T.; Robock, A.; Stephens, G.; Takemura,
697 T.; Zhang, H. Anthropogenic and Natural Radiative Forcing Supplementary Material. In *The*
698 *Physical Science Basis. Contribution of Working Group I to the Fifth Assessment Report of the*
699 *Intergovernmental Panel on Climate Change*. Cambridge University Press; Stocker, T. F.,
700 Qin, D., Plattner, G.-K., Tignor, M., Allen, S. K., Boschung, J., Nauels, A., Xia, Y., Bex, V.,
701 Midgley, P. M., Eds.; Cambridge University Press, Cambridge, United Kingdom and New
702 York, NY, USA., 2013.
- 703 (66) Forster, P.; Ramaswamy, V.; Artaxo, P.; Bernsten, T.; Betts, R.; Fahey, D. W.; Haywood, J.;
704 Lean, J.; Lowe, D. C.; Myhre, G.; Nganga, J.; Prinn, R.; G. Raga, M. S. and R. V. D. Changes
705 in Atmospheric Constituents and in Radiative Forcing. In *Climate Change 2007: The Physical*
706 *Science Basic. Contribution of Working Group I to the Fourth Assessment Report of the*
707 *Intergovernmental Panel on Climate Change*. Cambridge University Press; Solomon, S., Qin,
708 D., Manning, M., Chen, Z., Marquis, M., Averyt, K. B., Tignor, M., Miller, H. L., Eds.;
709 Cambridge University Press, Cambridge, United Kingdom and New York, NY, USA., 2007.
- 710 (67) Shine, K. P.; Bernsten, T. K.; Fuglestedt, J. S.; Skeie, R. B.; Stuber, N. Comparing the
711 Climate Effect of Emissions of Short- and Long-Lived Climate Agents. *Philos. Trans. R. Soc.*
712 *A Math. Phys. Eng. Sci.* **2007**, 365 (1856), 1903–1914. <https://doi.org/10.1098/rsta.2007.2050>.
- 713 (68) SCRIPPS. Atmospheric CO2 Data, Primary Mauna Loa CO2 Record. Scripps Institution of
714 Oceanography. http://scrippsco2.ucsd.edu/data/atmospheric_co2/primary_mlo_co2_record
715 (accessed Feb 23, 2019).
- 716 (69) Joos, F.; Roth, R.; Fuglestedt, J. S.; Peters, G. P.; Enting, I. G.; Von Bloh, W.; Brovkin, V.;
717 Burke, E. J.; Eby, M.; Edwards, N. R.; Friedrich, T.; Frölicher, T. L.; Halloran, P. R.; Holden,
718 P. B.; Jones, C.; Kleinen, T.; Mackenzie, F. T.; Matsumoto, K.; Meinshausen, M.; Plattner, G.
719 K.; Reisinger, A.; Segschneider, J.; Shaffer, G.; Steinacher, M.; Strassmann, K.; Tanaka, K.;
720 Timmermann, A.; Weaver, A. J. Carbon Dioxide and Climate Impulse Response Functions for
721 the Computation of Greenhouse Gas Metrics: A Multi-Model Analysis. *Atmos. Chem. Phys.*
722 **2013**, 13 (5), 2793–2825. <https://doi.org/10.5194/acp-13-2793-2013>.
- 723 (70) Levasseur, A.; Lesage, P.; Margni, M.; Deschênes, L.; Samson, R. Considering Time in LCA:
724 Dynamic LCA and Its Application to Global Warming Impact Assessments. *Environ. Sci.*
725 *Technol.* **2010**, 44 (8), 3169–3174. <https://doi.org/10.1021/es9030003>.
- 726 (71) Schwietzke, S.; Griffin, W. M.; Matthews, H. S. Relevance of Emissions Timing in Biofuel

- 727 Greenhouse Gases and Climate Impacts. *Environ. Sci. Technol.* **2011**, *45* (19), 8197–8203.
- 728 (72) Hudson, S. R. Estimating the Global Radiative Impact of the Sea Ice Albedo Feedback in the
729 Arctic. *J. Geophys. Res.* **2011**, *116* (D16), D16102-. <https://doi.org/10.1029/used>.
- 730 (73) Jackson, L. C.; Kahana, R.; Graham, T.; Ringer, M. A.; Woollings, T.; Mecking, J. V.; Wood,
731 R. A. Global and European Climate Impacts of a Slowdown of the AMOC in a High
732 Resolution GCM. *Clim. Dyn.* **2015**, *45* (11–12), 3299–3316. [https://doi.org/10.1007/s00382-](https://doi.org/10.1007/s00382-015-2540-2)
733 [015-2540-2](https://doi.org/10.1007/s00382-015-2540-2).
- 734 (74) Vellinga, M.; Wood, R. A. Impacts of Thermohaline Circulation Shutdown in the Twenty-First
735 Century. *Clim. Change* **2008**, *91* (1–2), 43–63. <https://doi.org/10.1007/s10584-006-9146-y>.
- 736 (75) Kuhlbrodt, T.; Rahmstorf, S.; Zickfeld, K.; Vikebø, F. B.; Sundby, S.; Hofmann, M.; Link, P.
737 M.; Bondeau, A.; Cramer, W.; Jaeger, C. An Integrated Assessment of Changes in the
738 Thermohaline Circulation. *Clim. Change* **2009**, *96* (4), 489–537.
739 <https://doi.org/10.1007/s10584-009-9561-y>.
- 740 (76) Meinshausen, M.; Wigley, T. M. L.; Raper, S. C. B. Emulating Atmosphere-Ocean and
741 Carbon Cycle Models with a Simpler Model , MAGICC6 – Part 2 : Applications. *Atmos.*
742 *Chem. Phys.* **2011**, *11*, 1457–1471. <https://doi.org/10.5194/acp-11-1457-2011>.
- 743 (77) JRC. *International Reference Life Cycle Data System (ILCD) Handbook -- General Guide for*
744 *Life Cycle Assessment -- Detailed Guidance. Luxembourg. Publications Office of the*
745 *European Union; Ispra, 2010.*
- 746 (78) Jolliet, O.; Antón, A.; Boulay, A.; Cherubini, F.; Fantke, P.; Levasseur, A.; Mckone, T. E.;
747 Michelsen, O.; Milà, L.; Motoshita, M. Global Guidance on Environmental Life Cycle Impact
748 Assessment Indicators : Impacts of Climate Change , Fine Particulate Matter Formation ,
749 Water Consumption and Land Use. *Int. J. Life Cycle Assess.* **2018**, *23*, 2189–2207.
- 750 (79) Levasseur, A.; Lesage, P.; Margni, M.; Samson, R. Biogenic Carbon and Temporary Storage
751 Addressed with Dynamic Life Cycle Assessment. *J. Ind. Ecol.* **2012**, *17* (1), 117–128.
752 <https://doi.org/10.1111/j.1530-9290.2012.00503.x>.
- 753 (80) Ishigaki, T.; Sugano, W.; Nakanishi, A.; Tateda, M.; Ike, M.; Fujita, M. The Degradability of
754 Biodegradable Plastics in Aerobic and Anaerobic Waste Landfill Model Reactors.
755 *Chemosphere* **2004**, *54*, 225–233. [https://doi.org/10.1016/S0045-6535\(03\)00750-1](https://doi.org/10.1016/S0045-6535(03)00750-1).
- 756 (81) Cho, H. S.; Moon, H. S.; Kim, M.; Nam, K.; Kim, J. Y. Biodegradability and Biodegradation
757 Rate of Poly (Caprolactone) -Starch Blend and Poly (Butylene Succinate) Biodegradable
758 Polymer under Aerobic and Anaerobic Environment. *Waste Manag.* **2011**, *31* (3), 475–480.

- 759 <https://doi.org/10.1016/j.wasman.2010.10.029>.
- 760 (82) Tansel, B. Persistence Times of Refractory Materials in Landfills: A Review of Rate Limiting
761 Conditions by Mass Transfer and Reaction Kinetics. *J. Environ. Manage.* **2019**, *247*
762 (February), 88–103. <https://doi.org/10.1016/j.jenvman.2019.06.056>.
- 763 (83) Rossi, V.; Cleeve-Edwards, N.; Lundquist, L.; Schenker, U.; Dubois, C.; Humbert, S.; Jolliet,
764 O. Life Cycle Assessment of End-of-Life Options for Two Biodegradable Packaging
765 Materials: Sound Application of the European Waste Hierarchy. *J. Clean. Prod.* **2015**, *86*,
766 132–145. <https://doi.org/10.1016/j.jclepro.2014.08.049>.
- 767
- 768
- 769
- 770